

NEW SIMPLE AND ACCURATE QUINTESSENCE APPROXIMATIONS

ARTUR ALHO,^{1*} AND CLAES UGGLA,^{2†}

¹*Center for Mathematical Analysis, Geometry and Dynamical Systems,
Instituto Superior Técnico, Universidade de Lisboa,*

Av. Rovisco Pais, 1049-001 Lisboa, Portugal.

²*Department of Physics, Karlstad University,
S-65188 Karlstad, Sweden.*

Abstract

We derive new approximations for quintessence solutions that are simpler and an order of magnitude more accurate than anything available in the literature, which from an observational perspective *makes numerical calculations superfluous*. For example, our tracking quintessence approximation yields $\sim 0.1\%$ maximum relative errors of $H(z)/H_0$ and $\Omega_m(z)$ for the observationally viable inverse power law scalar field potentials, and similarly for viable thawing quintessence models using two slow-roll parameters. The approximations are trivially computed from the scalar field potential and as an application we give *analytic* expressions for the CPL parameters calculated from an arbitrary scalar field potential for thawing and tracking quintessence models.

*Electronic address: aalho@math.ist.utl.pt

†Electronic address: claes.uggla@kau.se

1 Introduction

A growing number of increasingly precise cosmological observations of, e.g., type Ia supernovae [1, 2, 3], the cosmic microwave background (CMB) [4], various measurements of the Hubble parameter [5, 6, 7], the universe large-scale structure (LSS) and baryon acoustic oscillations (BAO) [8, 9, 10, 11, 12, 13, 14, 15], suggest that the universe is presently accelerating. In addition cosmological observations indicate that most of the matter in the universe is invisible ‘dark matter’ [16, 17, 18, 19]. The standard interpretation of the observations rely on that General Relativity is an accurate description of gravity on cosmological scales and that the observable Universe is almost spatially homogeneous, isotropic and flat on sufficiently large spatial scales. This leads to that the acceleration of the universe requires a ‘dark energy’ (DE) density component, ρ_{DE} , with sufficiently large negative pressure, while the dark matter seems to be best described by a dominant cold dark matter (CDM) energy density component, ρ_{m} , without pressure. The simplest model that is compatible with these assumptions is the Λ CDM model, for which the energy density ρ_{DE} and pressure p_{DE} are given by $\rho_{\text{DE}} = -p_{\text{DE}} = \Lambda > 0$, where Λ is the cosmological constant.

There are, however, theoretical problems, e.g., the nature of dark matter [20, 21], the observed small value of Λ and the coincidence problem, see e.g. [22] and references therein. Recent tensions between some data sets [23, 24, 25] and that large scale structures seem to form surprisingly early in the universe [26] have further aggravated the situation, which has contributed as motivation for numerous dynamical DE models for which ρ_{DE} is evolving. Many of these models are purely cosmographically motivated, without any tie to any theory, notably the Chevallier-Polarski-Linder (CPL) parametrization [27, 28] of the DE equation of state parameter $w_{\text{DE}} = p_{\text{DE}}/\rho_{\text{DE}}$ and a plethora of variations thereof, see e.g. [29] and references therein.

Some DE models, however, endeavour to have some theoretical motivation, where one of the simplest attempts is quintessence, i.e. a canonical scalar field, ϕ , minimally coupled to gravity, see e.g. [30] and [31] for references. This is the topic of the present paper, which deals with a non-interacting scalar field and matter in a spatially homogeneous, isotropic and flat spacetime, although note that the ideas in this paper are applicable to many other models and alternative theories. More specifically, we will *derive* simple, *analytic*, and accurate approximations for thawing quintessence, which exists for all scalar field potentials, and tracking quintessence for asymptotically inverse power-law potentials, i.e. $V \propto \phi^{-p}$, $p > 0$ when $\phi \rightarrow 0$ (i.e. the types of quintessence that dominate the observational literature).¹ Notably, our best approximations are typically *simpler and an order of magnitude more accurate than anything available in the literature*. For example, our tracking quintessence approximation yields $\sim 0.1\%$ maximum relative errors for $H(z)/H_0$ and $\Omega_{\text{m}}(z)$ for observationally viable inverse power law scalar field potentials, and similarly for viable thawing quintessence models using two slow-roll parameters. We note that from an observational perspective the remarkable accuracy of *our approximations makes numerical calculations superfluous when assessing observational constraints*; moreover the approximations yield an analytic overview of the observational viability of broader ranges of models than those that are typically numerically investigated.

¹Different types and nomenclatures for quintessence are discussed in section 3.

The accuracy and scope of our approximations have far ranging consequences. There are many papers that start from specific scalar field potentials and numerically compute observational consequences for a variety of initial data, often not particularly numerically systematically explored. For a wide range of scalar field potentials the present paper makes numerical explorations mote. Although there are mathematical considerations in this paper that might be unfamiliar to people in this field, the results are very easy to understand. For the reader not interested in the derivation of the approximations and only wants to use the results, just plug in your favourite potential into our *master equations*: for *thawing quintessence* use eq. (47) to obtain approximations for $w_\phi(z)$, $\Omega_\phi(z)$ (or, equivalently, $\Omega_m(z) = 1 - \Omega_\phi(z)$) and $H(z)$, where z is the redshift, while eq. (69) yields analytic expressions for the CPL parameters, thereby obtaining simple, accurate, analytical descriptions of the recent analysis of Wolf and Ferreira [32] and by Shlivko and Steinhardt [33], where one can also broaden the range of models; for *tracking quintessence* use eqs. (57) and (58) to obtain approximations for $w_\phi(z)$, $\Omega_\phi(z)$ (or, equivalently, $\Omega_m(z) = 1 - \Omega_\phi(z)$) and $H(z)$, while eq. (69) gives analytic expressions for the CPL parameters.

The outline of the paper is as follows. The next section provides a unifying general DE context for some of the structures that thawing and tracking quintessence share. In Section 3 we derive the expressions for the parameters appearing in the previous DE section that are particular for thawing and tracking quintessence, respectively. In addition, we explicitly give the simple analytical expressions for $w_\phi(z)$, $\Omega_\phi(z)$ (or, equivalently $\Omega_m(z) = 1 - \Omega_\phi(z)$) and $H(z)$. Section 4 gives explicit analytical expressions for the CPL parameters based on our new extremely accurate approximations. From an observational standpoint, this eliminates the need for numerical calculations of the CPL parameters for whatever potential one might be interested in, which is how one traditionally computes them for quintessence, see e.g. [32, 33]. Section 5 compares the new thawing and tracking quintessence approximations with numerical calculations and previous approximations in the literature, reviewed in Appendix A. The main part of the paper ends with section 6, which includes suggestions for future applications of the present approach and results. Appendix B deals with scaling freezing quintessence (the remaining type of quintessence not covered in the main part of the paper since $\lim_{z \rightarrow \infty} \Omega_\phi > 0$ in this case, which is in contrast to thawing and tracking quintessence for which $\lim_{z \rightarrow \infty} \Omega_\phi = 0$).

2 Common thawing and tracking quintessence considerations

In this section we will consider rather general aspects of dark energy that cover some features that are common for both thawing and tracking quintessence, which we treat individually in section 3.

2.1 Preliminaries

Spatially homogeneous, isotropic and flat spacetimes have a line element that can be written as²

$$\begin{aligned} ds^2 &= -dt^2 + a^2(t)\delta_{ij}dx^i dx^j \\ &= (1+z)^{-2} [H^{-2}(z)dz^2 + a_0^2\delta_{ij}dx^i dx^j], \end{aligned} \quad (1)$$

where $a(t)$ is the cosmological scale factor, $a_0 = a(t_0)$ (throughout, a subscript $_0$ refers to quantities at the present time $t = t_0$), where a_0 is usually set to one by an appropriate scaling of the spatial coordinates;

$$H = \frac{\dot{a}}{a} \quad (2)$$

denotes the Hubble parameter, where the dot refers to differentiation with respect to the cosmic time t , while $z = (a_0/a) - 1$ is the redshift.

Since the spacetime is described by the Hubble parameter $H(z)$ it follows that cosmological observables and their interpretation depend directly on $H(z)$, its derivatives and integrals. This is illustrated by, e.g., the deceleration parameter $q = -a\ddot{a}/\dot{a}^2 = -1 + (1+z)\frac{dH}{dz}/H$, and many distance measures, e.g., the Hubble distance $D_H(z)$, the proper motion or coordinate distance $D_M(z)$, the luminosity distance $D_L(z)$, the angular diameter distance $D_A(z)$, which are given by (see, e.g. [29])

$$D_H = \frac{1}{H(z)}, \quad (3a)$$

$$D_M = \int_0^z H^{-1}(\tilde{z})d\tilde{z}, \quad (3b)$$

$$D_L = (1+z) \int_0^z H^{-1}(\tilde{z})d\tilde{z}, \quad (3c)$$

$$D_A = (1+z)^{-1} \int_0^z H^{-1}(\tilde{z})d\tilde{z}. \quad (3d)$$

To find interesting alternatives to Λ CDM some authors simply choose some $H(z)$, e.g. H^2 being a polynomial in $1+z$ as in [29], or obtain $H(z)$ by assuming a specific form for one of the distance measures, e.g. $D_L(z)$, which yield $H(z)$ via $d[D_L(z)/(1+z)]/dz = 1/H(z)$, see e.g. [29]. More commonly, however, is to make a choice of the DE equation of state parameter

$$w_{\text{DE}} = \frac{p_{\text{DE}}}{\rho_{\text{DE}}} \quad (4)$$

that is different than the Λ CDM value $w_{\text{DE}} = -1$ (see e.g. [25] and references therein for a plethora of examples of $w_{\text{DE}}(z)$ and $w_{\text{DE}}(a)$). Note, however, that w_{DE} is not a physical observable. Since cosmological observations depend on $H(z)$, it is necessary to compute $H(z)$ from $w_{\text{DE}}(z)$, which requires the Einstein field equations and the matter conservation equations.

²We use units such that $c = 1$ and $8\pi G = 1$, where c is the speed of light and G is the gravitational constant.

Although the distance measures are naturally expressed in terms of the redshift z , computations are usually simpler using the e -fold time $N = \ln(a/a_0)$, where it is subsequently trivial to transform results to the redshift z by using the relation

$$1 + z = \exp(-N). \quad (5)$$

For simplicity we consider only non-interacting pressure free matter and a dark energy component.³ The matter conservation equations for the matter energy density, $\rho_m > 0$ and the DE energy density, $\rho_{\text{DE}} > 0$, are given by

$$\rho'_m = -3\rho_m \quad \Rightarrow \quad \rho_m = \rho_{m0} \exp(-3N), \quad (6a)$$

$$\rho'_{\text{DE}} = -3(1 + w_{\text{DE}})\rho_{\text{DE}} \quad \Rightarrow \quad \rho_{\text{DE}} = \rho_{\text{DE}0} \exp(-3N)f(N), \quad (6b)$$

where a $'$ denotes the derivative with respect to N and where $f(N)$ is defined as

$$f = \exp\left(-3 \int_0^N w_{\text{DE}}(\tilde{N})d\tilde{N}\right). \quad (7)$$

2.2 Relationships between Ω_{DE} , Ω_m , w_{DE} and H

Next we introduce the dimensionless and bounded Hubble-normalized variables Ω_{DE} and Ω_m :

$$\Omega_{\text{DE}} = \frac{\rho_{\text{DE}}}{3H^2} = \frac{\rho_{\text{DE}}}{\rho}, \quad \Omega_m = \frac{\rho_m}{3H^2} = \frac{\rho_m}{\rho}, \quad (8)$$

where we have used the Friedmann equation (i.e. the Gauss constraint)

$$3H^2 = \rho = \rho_m + \rho_{\text{DE}}, \quad (9)$$

which yields

$$\Omega_m + \Omega_{\text{DE}} = 1 \quad \Rightarrow \quad \Omega_{m0} + \Omega_{\text{DE}0} = 1. \quad (10)$$

To display the relationship between these quantities and H it is convenient to introduce the present time normalized Hubble parameter

$$E = \frac{H}{H_0}. \quad (11)$$

Equations (9), (6) and (8) result in the following DE expression for $E^2 = E_{\text{DE}}^2$:

$$E_{\text{DE}}^2 = \Omega_{m0} \exp(-3N) + \Omega_{\text{DE}0} \exp(-3N)f(N). \quad (12)$$

Using $\rho_{\text{DE}}/\rho_m = \Omega_{\text{DE}}/\Omega_m = \Omega_{\text{DE}}/(1 - \Omega_{\text{DE}})$ and (6), (10) yield

$$\Omega_{\text{DE}} = \frac{\Omega_{\text{DE}0}}{[\Omega_{m0}/f(N)] + \Omega_{\text{DE}0}}, \quad \Omega_m = \frac{\Omega_{m0}}{\Omega_{m0} + \Omega_{\text{DE}0}f(N)}. \quad (13)$$

Since the above expressions involve $f(N)$, the integral (7) needs to be computed from $w_{\text{DE}}(N)$.

³Although the gravitational influence of radiation is negligible when quintessence is important for the evolution of the Universe, we will comment on how to add it to our approximations in section 6.

If one instead of $w_{\text{DE}}(N)$ has $\Omega_{\text{DE}}(N)$ (or $\Omega_{\text{m}}(N) = 1 - \Omega_{\text{DE}}(N)$), then one can obtain $w_{\text{DE}}(N)$ and $E_{\text{DE}}^2(N)$ from $\Omega_{\text{DE}}(N)$ since

$$w_{\text{DE}} = \frac{1}{3} \left[\ln \left(\frac{\Omega_{\text{m}}}{\Omega_{\text{DE}}} \right) \right]' = \frac{1}{3} \left[\ln \left(\frac{1 - \Omega_{\text{DE}}}{\Omega_{\text{DE}}} \right) \right]', \quad (14a)$$

$$E_{\text{DE}}^2 = \exp(-3N) \left(\frac{\Omega_{\text{m}0}}{\Omega_{\text{m}}} \right) = \exp(-3N) \left(\frac{1 - \Omega_{\text{DE}0}}{1 - \Omega_{\text{DE}}} \right) \quad (14b)$$

follows from (6) and (8).

We finally note that the deceleration parameter q is defined as

$$q = -\frac{a\ddot{a}}{\dot{a}^2} = -1 - \frac{H'}{H}, \quad (15)$$

and is related to the total equation of state parameter w_{tot} according to

$$1 + w_{\text{tot}} = \frac{2}{3}(1 + q), \quad (16)$$

where

$$w_{\text{tot}} = \frac{p}{\rho} = \frac{p_{\text{DE}}}{\rho} = w_{\text{DE}} \left(\frac{\rho_{\text{DE}}}{\rho} \right) = w_{\text{DE}} \Omega_{\text{DE}}. \quad (17)$$

To derive the above relations, we have used the Friedmann equation $\rho = 3H^2$ to obtain the last equality in (17), and also (15) and (6) to establish $\rho' = -3(1 + w_{\text{tot}})\rho$, which also follows from the Einstein field equations.

In the following sections we will discuss quintessence for which $w_{\text{DE}} = w_{\phi}$. As we will see, with the exception of ‘scaling freezing quintessence’ models, discussed in Appendix B, the evolution of the universe is described by ‘attractor’ solutions for which $\lim_{N \rightarrow -\infty} w_{\phi} = -1$ for thawing quintessence and $\lim_{N \rightarrow -\infty} w_{\phi} = w_{\infty} = \text{constant}$, $-1 < w_{\infty} < 0$ for tracking quintessence for asymptotically inverse power law potentials. Thus, the evolution toward the past of these solutions is described by the Λ CDM and w CDM models, respectively. Let us therefore recall the properties of these models.

2.3 The Λ CDM and w CDM models

The Λ CDM and the w CDM models are characterized by $w_{\text{DE}} = -1$ and $w_{\text{DE}} = \text{constant} = w$, respectively. This leads to that (7) results in

$$f = e^{3N} \quad \text{and} \quad f = e^{-3wN}, \quad (18)$$

respectively, where (13) and (12) then yield

$$\Omega_{\Lambda} = \frac{\Omega_{\Lambda 0}}{\Omega_{\text{m}0}e^{-3N} + \Omega_{\Lambda 0}}, \quad \Omega_w = \frac{\Omega_{w0}}{\Omega_{\text{m}0}e^{3wN} + \Omega_{w0}}, \quad (19a)$$

$$E_{\Lambda}^2 = \Omega_{\text{m}0}e^{-3N} + \Omega_{\Lambda 0}, \quad E_w^2 = \Omega_{\text{m}0}e^{-3N} + \Omega_{w0}e^{-3(1+w)N}, \quad (19b)$$

where we use the subscripts $_{\Lambda}$ and $_w$ to characterize the Λ CDM and w CDM expressions for Ω_{DE} and E_{DE}^2 , respectively.

2.4 Past DE series expansions

Equation (14a) can be written as

$$\Omega'_{\text{DE}} = -3w_{\text{DE}}\Omega_{\text{DE}}(1 - \Omega_{\text{DE}}). \quad (20)$$

As we will see, thawing quintessence and tracking quintessence are associated with $\lim_{N \rightarrow -\infty} w_\phi = w_\infty = -1$ and $\lim_{N \rightarrow -\infty} w_\phi = w_\infty = \text{constant} \in (-1, 0)$, respectively. To derive some common features of these two types of quintessence, we therefore assume that

$$w_\infty = \lim_{N \rightarrow -\infty} w_{\text{DE}} = \text{constant} \in [-1, 0), \quad (21)$$

which in combination with (20) yields

$$\lim_{N \rightarrow -\infty} \Omega_{\text{DE}} = 0. \quad (22)$$

Thus, $\lim_{N \rightarrow -\infty} \Omega_{\text{m}} = 1$, i.e. the asymptotic past is matter dominated. Equations (20), (21) and (22) lead to the approximation $\Omega'_{\text{DE}} \approx -3w_\infty\Omega_{\text{DE}}$ when $N \rightarrow -\infty$ and hence

$$\Omega_{\text{DE}} \approx Ce^{-3w_\infty N}. \quad (23)$$

Motivated by this, let us now consider w_{DE} and Ω_{DE} and perform series expansions in

$$T = T_0 e^{-3w_\infty N}, \quad (24)$$

where $T \rightarrow 0$ when $N \rightarrow -\infty$. If one starts with a series expansion in w_{DE} and uses (7) and (13) one obtains an expression for Ω_{DE} that subsequently can be series expanded in T ; on the other hand, if one starts with a series expansion in Ω_{DE} and inserts this into (14a) one obtains an expression for w_{DE} that one then can series expand in T . These two procedures result in the same series expansions, which can be written as⁴

$$w_{\text{DE}} = w_\infty [1 - (\gamma - 1)T + (\gamma - 1)\beta T^2 + \dots] \quad (25a)$$

$$\Omega_{\text{DE}} = T \left(1 - \gamma T + \left[1 + \frac{1}{2}(\gamma - 1)(3 + \gamma + \beta) \right] T^2 + \dots \right). \quad (25b)$$

2.5 DE Padé approximants and present initial data

For brevity we will restrict our considerations by following the most common approach in the literature, which is to use w_{DE} as the starting point. Next we will transform the series expansion for w_{DE} in T to Padé approximants for two reasons:

- (i) To obtain *exact* DE models that naturally generalize the Λ CDM and w CDM models and at the same time form a unifying DE context for some of the structures that thawing and tracking quintessence share. Moreover, the Padé approximants create a link between the past and the present day initial data $\rho_{\text{m}0}$ and H_0 via $\Omega_{\text{DE}0} = 1 - \Omega_{\text{m}0} = 1 - \rho_{\text{m}0}/3H_0^2$. This section thereby forms a unifying starting point for the quintessence approximations in the next section.

⁴The given expressions can be generalized by writing $w_{\text{DE}} = w_\infty [1 + \alpha T + \sigma T^2 + \dots]$, which subsequently can be used to compute the series expansions for Ω_{DE} and, e.g., E_{DE}^2 . The reason we have written α as $-(\gamma - 1)$ and σ as $(\gamma - 1)\beta$ is that this simplifies and is compatible with our quintessence approximations.

- (ii) The main point of the paper: To obtain sufficiently good *analytic* approximations to the solutions of the quintessence field equations so that numerical investigations of observational issues for thawing and tracking quintessence become unnecessary! This is accomplished by transforming the series expansions that approximate solutions to the quintessence equations in the next section toward the past to Padé approximants that also are accurate at the present time.⁵

Our first and second order expansions in T for w_{DE} yield the following Padé approximants for w_{DE} , respectively, which thereby serve as our DE models:

$$w_{\text{DE}} = [0/1]_{w_{\text{DE}}}(T) = \frac{w_{\infty}}{1 + (\gamma - 1)T}, \quad (26a)$$

$$w_{\text{DE}} = [1/1]_{w_{\text{DE}}}(T) = w_{\infty} \left(\frac{1 + [\beta - (\gamma - 1)]T}{1 + \beta T} \right) = w_{\infty} \left(1 - \frac{(\gamma - 1)T}{1 + \beta T} \right), \quad (26b)$$

where we recall that $T = T_0 e^{-3w_{\infty}N}$. Note that setting $\beta = \gamma - 1$ in $w_{\text{DE}} = [1/1]_{w_{\text{DE}}}(T)$ yields $w_{\text{DE}} = [0/1]_{w_{\text{DE}}}(T)$ (and similarly for the expressions below for Ω_{DE} and E_{DE} that follow from $w_{\text{DE}} = [1/1]_{w_{\text{DE}}}(T)$). Furthermore, setting $\gamma = 1$ results in $w_{\text{DE}} = w_{\infty}$ and hence ΛCDM when $w_{\infty} = -1$ and $w\text{CDM}$ when $-1 < w_{\infty} < 0$.

To connect with initial data at the present time we can set $N = 0$ and solve for $T(0) = T_0$ in (26) in terms of the left hand side $w_{\text{DE}}(0) = w_{\text{DE}0}$. Since results obtained from (26a) can be obtained from the corresponding ones obtained from (26b) by setting $\beta = \gamma - 1$ we now focus on the latter. It follows from (26b) and (7) that the $[1/1]_{w_{\text{DE}}}(T)$ approximant yields

$$T_0 = \frac{\frac{w_{\infty}}{w_{\text{DE}0}} - 1}{\beta - \frac{w_{\infty}}{w_{\text{DE}0}} [\beta - (\gamma - 1)]}, \quad (27a)$$

$$w_{\text{DE}} = w_{\infty} \left(1 - \frac{(\gamma - 1) \left(\frac{w_{\infty}}{w_{\text{DE}0}} - 1 \right) e^{-3w_{\infty}N}}{\beta - \frac{w_{\infty}}{w_{\text{DE}0}} [\beta - (\gamma - 1)] + \beta \left(\frac{w_{\infty}}{w_{\text{DE}0}} - 1 \right) e^{-3w_{\infty}N}} \right), \quad (27b)$$

$$f = e^{-3w_{\infty}N} \left(\frac{(\gamma - 1) \frac{w_{\infty}}{w_{\text{DE}0}}}{\beta - \frac{w_{\infty}}{w_{\text{DE}0}} [\beta - (\gamma - 1)] + \beta \left(\frac{w_{\infty}}{w_{\text{DE}0}} - 1 \right) e^{-3w_{\infty}N}} \right)^{\frac{\gamma-1}{\beta}}, \quad (27c)$$

where f yields Ω_{DE} , Ω_{m} and E_{DE} via (13) and (12). As pointed out previously, the corresponding expressions obtained from the $[0/1]_{w_{\text{DE}}}(T)$ approximant are conveniently obtained from the results in (27) by setting $\beta = \gamma - 1$.

We note, however, that $w_{\text{DE}0}$ is not an observable. It is determined by $\Omega_{\text{DE}0}$ and $\Omega'_{\text{DE}}|_{N=0}$ (or $\frac{\Omega_{\text{DE}}}{dz}|_{z=0}$) via eq. (14a), which is not an easy observational task. For this reason we will instead relate T_0 to $\Omega_{\text{DE}0}$ and thereby obtain a direct connection to the observables H_0 and $\rho_{\text{m}0}$ since $1 - \Omega_{\text{DE}0} = \Omega_{\text{m}0} = \rho_{\text{m}0}/3H_0^2$. We therefore consider the $[1/1]_{\Omega_{\text{DE}}}(T)$ Padé approximant for Ω_{DE} (use the expression (25b) up to second order in T):

$$\Omega_{\text{DE}} = [1/1]_{\Omega_{\text{DE}}}(T) = \frac{T}{1 + \gamma T}, \quad (28)$$

⁵It is quite common to use Padé approximants to improve convergence in a wide range of contexts, e.g. to obtain accurate approximations for solutions to differential equations; for a brief review, references, and applications in a cosmological setting, see, e.g., [34].

from which it follows that $\Omega_{\text{DE}0} = T_0/[1 + \gamma T_0]$, which results in

$$T_0 = \frac{\Omega_{\text{DE}0}}{1 - \gamma\Omega_{\text{DE}0}}. \quad (29)$$

This is then inserted into (26a), which when used in (7) to obtain $f(N)$ leads to the same expression as (28) with (29) inserted. At the prize of additional complexity, one can continue to produce Padé approximants for Ω_{DE} that also involve the higher order term with β in the expansion.⁶ This, however, leads to that expressing T_0 in terms of $\Omega_{\text{DE}0}$ requires solving quadratic equations in T_0 , which leads to rather messy expressions. The approximation (28) turns out to be a fairly good approximation for quintessence. For this reason we will use the simple result in (29) for T_0 in (26b). This leads to that the expressions for w_{DE} in (26) can be written as follows:⁷

$$w_{\text{DE}} = [0/1]_{w_{\text{DE}}}(T) = w_\infty \left(1 - \frac{(\gamma - 1)\Omega_{\text{DE}0}}{(\gamma - 1)\Omega_{\text{DE}0} + (1 - \gamma\Omega_{\text{DE}0})e^{3w_\infty N}} \right), \quad (30a)$$

$$w_{\text{DE}} = [1/1]_{w_{\text{DE}}}(T) = w_\infty \left(1 - \frac{(\gamma - 1)\Omega_{\text{DE}0}}{\beta\Omega_{\text{DE}0} + (1 - \gamma\Omega_{\text{DE}0})e^{3w_\infty N}} \right), \quad (30b)$$

which result in the following present time values

$$w_{\text{DE}0} = w_\infty \left(\frac{1 - \gamma\Omega_{\text{DE}0}}{\Omega_{\text{m}0}} \right), \quad (31a)$$

$$w_{\text{DE}0} = w_\infty \left(1 - \frac{(\gamma - 1)\Omega_{\text{DE}0}}{1 + (\beta - \gamma)\Omega_{\text{DE}0}} \right). \quad (31b)$$

Inserting the expressions for $[0/1]_{w_{\text{DE}}}(T)$ and $[1/1]_{w_{\text{DE}}}(T)$ in (26) and (30) into (7) yields

$$\begin{aligned} f &= \frac{T}{T_0} \left(\frac{1 + (\gamma - 1)T_0}{1 + (\gamma - 1)T} \right) = \left(\frac{\Omega_{\text{m}0}}{\Omega_{\text{DE}0}} \right) \left(\frac{T}{1 + (\gamma - 1)T} \right) \\ &= \frac{\Omega_{\text{m}0}e^{-3w_\infty N}}{1 - \gamma\Omega_{\text{DE}0} + (\gamma - 1)\Omega_{\text{DE}0}e^{-3w_\infty N}}, \end{aligned} \quad (32a)$$

$$f = \frac{T}{T_0} \left(\frac{1 + \beta T_0}{1 + \beta T} \right)^{\frac{\gamma-1}{\beta}} = e^{-3w_\infty N} \left(\frac{1 + (\beta - \gamma)\Omega_{\text{DE}0}}{1 - \gamma\Omega_{\text{DE}0} + \beta\Omega_{\text{DE}0}e^{-3w_\infty N}} \right)^{\frac{\gamma-1}{\beta}}, \quad (32b)$$

where the first f comes from $[0/1]_{w_{\text{DE}}}(T)$ and the second from $[1/1]_{w_{\text{DE}}}(T)$.

It follows from (13) and (12) that the $[1/1]_{w_{\text{DE}}}(T)$ Padé approximant results in

$$\Omega_{\text{DE}} = \frac{\Omega_{\text{DE}0}}{\Omega_{\text{m}0}e^{3w_\infty N} \left(\frac{1 + \beta T}{1 + \beta T_0} \right)^{\frac{\gamma-1}{\beta}} + \Omega_{\text{DE}0}}, \quad (33a)$$

$$E_{\text{DE}}^2 = \Omega_{\text{m}0}e^{-3N} + \Omega_{\text{DE}0}e^{-3(1+w_\infty)N} \left(\frac{1 + \beta T_0}{1 + \beta T} \right)^{\frac{\gamma-1}{\beta}} \quad (33b)$$

⁶The next two higher order Padé approximants, which involve β , are given by $[1/2]_{\Omega_{\text{DE}}}(T) = \frac{T}{1 + \gamma T - \frac{1}{2}(\gamma-1)[1 + (\beta-\gamma)]T^2}$ and $[2/1]_{\Omega_{\text{DE}}}(T) = \frac{\gamma T + \frac{1}{2}(\gamma-1)[1 + (\beta-\gamma)]T^2}{\gamma + [1 + \frac{1}{2}(\gamma-1)(3 + \beta + \gamma)]T}$.

⁷Note that one can use the series expansion in T for Ω_{DE} to obtain the following expression for E_{DE}^2 : $E_{\text{DE}}^2 \approx \Omega_{\text{m}0} \exp(-3N)[1 + T - (\gamma - 1)T^2(1 + \frac{1}{2}(\gamma - 1 + \beta)T) + \dots]$ and use (29) for T_0 . This expression can subsequently be used to obtain various Padé approximants to obtain good quintessence approximations for $E_\phi(N)$ and then use $E_\phi(N)$ to compute, e.g., $w_\phi(N)$, if one is so inclined.

where we recall that $T = T_0 \exp(-3w_\infty N)$, $T_0 = \Omega_{\text{DE}0}/(1 - \gamma\Omega_{\text{DE}0})$, while the result for the $[0/1]_{w_{\text{DE}}}(T)$ Padé is obtained from the above expressions by setting $\beta = \gamma - 1$, which yields⁸

$$\Omega_{\text{DE}} = \frac{T}{1 + \gamma T} = \frac{\Omega_{\text{DE}0}}{\gamma\Omega_{\text{DE}0} + (1 - \gamma\Omega_{\text{DE}0})e^{3w_\infty N}}, \quad (34a)$$

$$\begin{aligned} E_{\text{DE}}^2 &= \Omega_{\text{m}0} e^{-3N} \left(1 + \frac{T}{1 + (\gamma - 1)T} \right) \\ &= \Omega_{\text{m}0} e^{-3N} \left(1 + \frac{\Omega_{\text{DE}0}}{(\gamma - 1)\Omega_{\text{DE}0} + (1 - \gamma\Omega_{\text{DE}0})e^{3w_\infty N}} \right). \end{aligned} \quad (34b)$$

Note the simple relationship between these expression and Λ CDM and w CDM, which are obtained by setting $\gamma = 1$. Furthermore, eq. (34a) implies the following relations between the models in (34) and Λ CDM and w CDM at the present time: $\Omega_{\text{DE}0} = \Omega_{\Lambda 0}/\gamma$ when $w_\infty = -1$ and $\Omega_{\text{DE}0} = \Omega_{w0}/\gamma$ when $w_\infty \in (-1, 0)$. As we shall see, thawing quintessence yields $\gamma > 1$; on the other hand, depending on the scalar field potential, there exist tracking quintessence models with $\gamma > 1$, $\gamma = 1$ and $\gamma < 1$.

Finally, note that it is trivial to express the above equations in the redshift z , since $z = \exp(-N) - 1$. The above may be interpreted as *exact cosmographic* DE models, but this is *not* what we are interested in. Our objective is to derive *approximations* for solutions of the field equations for *thawing and tracking quintessence*. This requires deriving γ and β from the quintessence field equations, which, of course, involves the scalar field potential; this is then followed by inserting the results for γ and β , expressed in terms of the scalar field potential and its derivatives, into the above DE formulas, which then are transformed from exact DE expressions to quintessence approximations.

3 Quintessence approximations

Before deriving expressions for the parameters γ and β for thawing and tracking quintessence, we begin with some background as regards quintessence. The concepts of thawing and freezing were defined by Caldwell and Linder (2005) [35] as follows: thawing is characterized by $w_\varphi \approx -1$ where w_φ subsequently grows, i.e. $w'_\varphi > 0$, while $w_\varphi > -1$ and $w'_\varphi < 0$ holds for freezing. Some quintessence models go through several stages of thawing and freezing, see e.g. [36], and sometimes thawing quintessence and freezing quintessence therefore refer to a quintessence model at the present time, but this is not always the case. Quintessence is associated with that there exist particular quintessence solutions to the field equations that attract open sets of other quintessence solutions. Once a solution has been attracted to an ‘attractor’ quintessence solution it shadows it and thereby share its properties. It should be noted that these open sets of non-attractor quintessence solutions have a pre-quintessence stage during the matter dominated epoch before they are attracted to an attractor quintessence solution. During this stage of evolution the scalar field is effectively a test field and therefore

⁸Note that by multiplying (34a) with γ it is easy to see that the transformation $\gamma\Omega_{\text{DE}} \rightarrow \Omega_w$ and $w_\infty \rightarrow w$ yields the expression in (19a), which specializes to Λ CDM when $w_\infty = -1$. In particular this leads to $\gamma\Omega_{\text{DE}0} = \Omega_{w0}$, which illustrates the danger of interpreting and transferring data from a w CDM or Λ CDM context to a different DE context.

not observationally relevant. To obtain an unambiguous nomenclature, we use the past asymptotic properties of the attractor solutions to denote the various types of quintessence.

For *all* scalar field potentials there is a 1-parameter set of thawing quintessence attractor solutions with $\phi = \phi_* = \text{constant}$, $w_\phi = -1$, $\Omega_m = 1$, $\Omega_\phi = 0$ when $N \rightarrow -\infty$; for asymptotically inverse power law potentials with $V \propto \phi^{-p}$, $p > 0$, when $\phi \rightarrow 0$, there is also a single tracker quintessence attractor solution with $-1 < w_\phi = -2/(2+p) < 0$, $\Omega_m = 1$, $\Omega_\phi = 0$ when $N \rightarrow -\infty$. For scalar field potentials that are sufficiently asymptotically exponentially steep there is a third type of quintessence: scaling freezing quintessence for which $w_\phi = 0$ when $p_m = 0$ and $0 < \Omega_m < 1$ when $N \rightarrow -\infty$. As a consequence this does not yield past continuous deformations of Λ CDM or w CDM and we will therefore only touch on this topic in appendix B. We thereby focus on thawing quintessence and tracking quintessence, which furthermore dominate what is observationally investigated in the literature. For more details and a rigorous global dynamical systems description of quintessence, see, e.g., [36], [37] and [38]. Next we derive dynamical systems that are adapted to obtaining the parameters γ and β for thawing and tracking quintessence, respectively.

3.1 Thawing quintessence

To obtain a dynamical system that is useful for deriving expressions for γ and β for thawing quintessence we introduce the following dimensionless bounded variable⁹

$$\Sigma_\phi = \frac{\phi'}{\sqrt{6}}, \quad (35)$$

and use $(\phi, \Sigma_\phi, \Omega_\phi)$ as the state vector together with the e -fold time N .¹⁰ To obtain a dynamical system for $(\phi, \Sigma_\phi, \Omega_\phi)$ we use (20) with $\Omega_{\text{DE}} = \Omega_\phi$ and that $w_{\text{DE}} = w_\phi$ is given by

$$w_\phi = -1 + \frac{2\Sigma_\phi^2}{\Omega_\phi}, \quad (36)$$

as follows from the definitions. In addition, the (non-linear) Klein-Gordon equation $\ddot{\phi} = -3H\dot{\phi} - V_{,\phi}$, expressed in e -fold time and Σ_ϕ , is needed. This leads to the dynamical system

$$\phi' = \sqrt{6}\Sigma_\phi, \quad (37a)$$

$$\Sigma'_\phi = -\frac{3}{2}(1 + \Omega_\phi - 2\Sigma_\phi^2)\Sigma_\phi + \sqrt{\frac{3}{2}}\lambda(\phi)(\Omega_\phi - \Sigma_\phi^2), \quad (37b)$$

$$\Omega'_\phi = 3(\Omega_\phi - 2\Sigma_\phi^2)(1 - \Omega_\phi), \quad (37c)$$

⁹The variable Σ_ϕ was first introduced by Coley *et al.* (1997) [39] and Copeland *et al.* (1998) [40] whose x is Σ_ϕ . Since then, Σ_ϕ (or ϕ') is commonly used to describe scalar fields in cosmology, see, e.g., Urena-Lopez (2012) [41], equation (2.3), Tsujikawa (2013) [30], equation (16) and Alho and Uggla (2015) [42], equation (8). The reason for using the notation Σ for the kernel is because Σ_ϕ plays a similar role as Hubble-normalized shear, which is typically denoted with the kernel Σ , see e.g. [43].

¹⁰The variables u and v in [36] yield slower convergence.

where we have introduced

$$\lambda(\phi) = -\frac{V_{,\phi}}{V}. \quad (38)$$

Since thawing quintessence begins in the matter dominated regime, $\Omega_m \approx 1$, when $w_\phi \approx -1$ initially, it follows from (36) and from $\Omega_m + \Omega_\phi = 1$ that thawing quintessence begins when $\Sigma_\phi^2 \ll \Omega_\phi \ll \Omega_m$. We then note that whenever $\lambda(\phi)$ is bounded, which always holds for some domain(s) of ϕ for *any* scalar field potential $V(\phi)$, there is a line of matter dominated ‘Friedmann-Lemaître’ fixed points in the present dynamical systems formulation given by

$$\text{FL}^{\phi_*}: \quad (\phi, \Sigma_\phi, \Omega_\phi) = (\phi_*, 0, 0) \quad (39)$$

and hence $\Omega_m = 1$, parametrized by the constant values ϕ_* . To determine what happens in the vicinity of FL^{ϕ_*} we linearize the equations at $(\phi, \Sigma_\phi, \Omega_\phi) = (\phi_*, 0, 0)$, which leads to

$$\phi \approx \phi_* + \frac{2\lambda_*}{9} C e^{3N} - \frac{2}{3} D e^{-\frac{3}{2}N}, \quad (40a)$$

$$\sqrt{6}\Sigma_\phi = \phi' \approx \frac{2\lambda_*}{3} C e^{3N} + D e^{-\frac{3}{2}N} \quad (40b)$$

$$\Omega_\phi \approx C e^{3N}, \quad (40c)$$

where $\lambda_* = \lambda(\phi_*)$. It follows that thawing quintessence is associated with the unstable manifold of FL^{ϕ_*} , obtained by setting $D = 0$. More precisely, thawing quintessence models consist of the 1-parameter set of unstable manifold orbits (i.e., solution trajectories) of FL^{ϕ_*} and the open set of orbits that intermediately shadows these orbits; this open set of orbits consists of the orbits that before the thawing epoch are pushed toward FL^{ϕ_*} by the stable manifold orbits of FL^{ϕ_*} and subsequently toward the unstable manifold orbits of FL^{ϕ_*} , which therefore approximate these orbits during their thawing stage of evolution, for details, see [36] and [38].

To find γ and β we Taylor expand $\lambda(\phi)$ around ϕ_* and make a series expansion in $T = T_0 e^{3N}$ for the variables $(\phi, \Sigma_\phi, \Omega_\phi)$. The coefficients in the expansion are found by inserting the expansions into the dynamical system (37) and solving for them. Truncation of the series in T gives

$$\phi \approx \phi_* + \sqrt{(\gamma - 1)/3} \left[T \left(1 - \frac{1}{2} \sigma T \right) \right], \quad (41a)$$

$$\sqrt{6}\Sigma_\phi = \phi' \approx \sqrt{3(\gamma - 1)} [T(1 - \sigma T)], \quad (41b)$$

$$\Omega_\phi \approx T \left[1 - \gamma T + \left(1 + (\gamma - 1) \left(\frac{3}{2} + \sigma \right) \right) T^2 \right], \quad (41c)$$

where γ and σ are related to the slow-roll parameters

$$\epsilon(\phi) = \frac{1}{2} \left(\frac{V_{,\phi}}{V} \right)^2 = \frac{\lambda^2}{2}, \quad \eta(\phi) = \frac{V_{,\phi\phi}}{V} = \lambda^2 - \lambda_{,\phi}, \quad (42)$$

computed at $\phi = \phi_*$ on FL^{ϕ_*} , i.e.,

$$\epsilon_* = \epsilon(\phi_*), \quad \eta_* = \eta(\phi_*), \quad (43)$$

according to

$$\gamma = 1 + \left(\frac{2}{3}\right)^3 \epsilon_*, \quad \sigma = \frac{4}{5} \left(1 + \frac{\eta_*}{6}\right); \quad (44)$$

where a comparison between (25b) and (41c) results in

$$\beta = \frac{3}{5} - \left(\frac{2}{3}\right)^3 \epsilon_* + \frac{4}{15} \eta_*. \quad (45)$$

Inserting the result for γ in (44) into (30a) and (34) yields our lowest order thawing quintessence approximations for w_ϕ , Ω_ϕ and E_ϕ , while inserting the results for γ in (44) and β in (45) into (30b) and (33) gives our corresponding most accurate approximations. Note that *these formulas are valid for any scalar field potential and any ϕ_** , but the approximations are only accurate for observationally viable solutions, i.e., models for which $\epsilon(\phi_*)$ and $\eta(\phi_*)$ are typically $\mathcal{O}(1)$ or less. Based on section 2 where we now replace the subscript DE with ϕ we obtain the following approximations for thawing quintessence: Throughout we use eq. (29) to connect with initial data, i.e.

$$T_0 = \frac{\Omega_{\phi 0}}{1 - \gamma \Omega_{\phi 0}}, \quad (46)$$

where $\Omega_{\phi 0}$ is observationally determined, which leads to that there is no error at all for our Ω_ϕ approximations at the present time,¹¹ although there will be small errors for both $w_{\phi 0}$ and $E_{\phi 0}$ from the $w_\phi \approx [1/1]_{\text{DE}}(T)$ based approximation, which we will focus on. On the other hand, computing $w_{\phi 0}$ *numerically* for one of the solutions from the 1-parameter set of thawing quintessence attractor solutions for a specific scalar field potential and using eq. (27a) for T_0 results, of course, in no deviation at all from the numerically calculated value for $w_{\phi 0}$.

Using that $w_\infty = -1$ for thawing quintessence leads to $T = T_0 \exp(3N)$ where we recall that $T_0 = \frac{\Omega_{\phi 0}}{1 - \gamma \Omega_{\phi 0}}$ (see e.q. (46)), while (30b) and (33) yield our *master equations for thawing quintessence*:

$$w_\phi \approx [1/1]_{w_{\text{DE}}}(T) = - \left(1 - \frac{(\gamma - 1)T}{1 + \beta T}\right), \quad (47a)$$

$$\Omega_\phi \approx \frac{\Omega_{\phi 0}}{\Omega_{\text{m}0} e^{-3N} \left(\frac{1 + \beta T}{1 + \beta T_0}\right)^{\frac{\gamma-1}{\beta}} + \Omega_{\phi 0}}, \quad (47b)$$

$$E_\phi^2 \approx \Omega_{\text{m}0} e^{-3N} + \Omega_{\phi 0} \left(\frac{1 + \beta T_0}{1 + \beta T}\right)^{\frac{\gamma-1}{\beta}}, \quad (47c)$$

where we recall that

$$\gamma = 1 + \left(\frac{2}{3}\right)^3 \epsilon_*, \quad (47d)$$

$$\beta = \frac{3}{5} - \left(\frac{2}{3}\right)^3 \epsilon_* + \frac{4}{15} \eta_*, \quad (47e)$$

¹¹A given value of $\Omega_{\phi 0}$ describes a surface in the state space $(\phi, \Sigma_\phi, \Omega_\phi)$. This surface determines where $N = 0$ for the various orbits in the state space.

where the slow-roll parameters ϵ_* and η_* are given by $\epsilon_* = \epsilon(\phi_*) = \frac{1}{2} (V_{,\phi}/V)^2|_{\phi=\phi_*}$ and $\eta_* = \eta(\phi_*) = V_{,\phi\phi}/V|_{\phi=\phi_*}$; the 1-parameter set of values ϕ_* are the freezing values of ϕ during the matter dominated regime where $\Omega_\phi \approx 0$, where each value yields a thawing quintessence attractor solution, where these solutions collectively describe an open set of solutions that shadow them during the epoch when quintessence affects the spacetime structure. The simpler, but less accurate approximations, although with similar accuracy as previous approximations in the literature, based on $w_\phi \approx [0/1]_{w_{\text{DE}}}(T)$, are obtained by setting $\beta = \gamma - 1$ in the above expressions. Recall also, that setting $\gamma = 1$, which corresponds to that $\epsilon_* = 0$, yields the Λ CDM solution. To express our approximations in the redshift z , just use the simple relation $z = \exp(-N) - 1$. The application of the above master equations is illustrated with a specific example, a quintessential α -attractor inflation potential, in section 5.

3.2 Tracking quintessence

Peebles and Ratra (1988) [44, 45] initiated the study of the inverse power law potential $V \propto \phi^{-p}$, $p > 0$. They obtained approximate expressions by assuming that H and ρ could be approximated by their values in the matter dominated regime and that the scale factor obeyed a power law dependence in cosmic time t . Subsequently Ratra and Quillen (1992) [46] obtained the asymptotic result $w_\phi = p_\phi/\rho_\phi = -2/(2+p)$ (their eq. (5)) for this potential. This work was then followed up by Zlatev *et al.* (1999) [47] and Steinhardt *et al.* (1999) [48],¹² who introduced the notation ‘tracker field’ as a form of quintessence, associated with potentials for which $\lambda \rightarrow \infty$ when $\phi \rightarrow 0$ and the condition $\Gamma > 1$, see also [30], where

$$\Gamma = \frac{V V_{,\phi\phi}}{V_{,\phi}^2} = 1 + (\lambda^{-1})_{,\phi}. \quad (48)$$

We are here considering asymptotically inverse power law potentials, characterized by

$$\lim_{\phi \rightarrow 0} \phi \lambda = p = \text{constant} > 0, \quad \lim_{\phi \rightarrow 0} \Gamma = 1 + \frac{1}{p}. \quad (49)$$

Next, we introduce a dynamical system that is suitable for deriving the parameters γ and β for tracking quintessence. Tracking quintessence for asymptotically inverse power law potentials requires that in the vicinity of $\phi = 0$ the potential and λ are monotonically decreasing, i.e., when $\lambda(\phi) > 0$ and $\Gamma(\phi) > 1$, as follows from (38) and (48). We now introduce a system of equations that are based on the following new variables:¹³

$$\tilde{\phi} = \lambda^{-2}(\phi), \quad u = \Sigma_\phi \sqrt{\frac{2}{\Omega_\phi}} = \frac{\phi'}{\sqrt{3\Omega_\phi}}, \quad v = \lambda(\phi) \sqrt{\frac{\Omega_\phi}{3}}, \quad (50)$$

¹²See also Podario and Ratra (2000) [49] and Peebles and Ratra (2003) [22].

¹³The variables $\tilde{\phi}$ and v are slightly different than the variables $\bar{\phi}$ and v in [37], which were adapted to a global state space setting, while the present ones are designed for fast convergence for the tracker orbit and the explicit appearance of Γ in the equations and results.

from which it follows, when taken together with (36),

$$1 + w_\phi = u^2, \quad \Omega_\phi = 3v^2\tilde{\phi}. \quad (51)$$

These variables lead to the dynamical system

$$\tilde{\phi}' = 6uv\tilde{\phi}(\Gamma(\tilde{\phi}) - 1), \quad (52a)$$

$$u' = \frac{3}{2}(2 - u^2)(v - u), \quad (52b)$$

$$v' = \frac{3}{2} \left[(1 - u^2)(1 - 3v^2\tilde{\phi}) - 2uv(\Gamma(\tilde{\phi}) - 1) \right] v, \quad (52c)$$

where we assume that $\Gamma(\tilde{\phi}) > 1$ is regular in $\tilde{\phi}$.

The dynamical system (52) admits $\tilde{\phi} = 0$ (and thereby $\phi = 0$) as an invariant boundary subset. As shown in [37], in regularizing variables, like the present ones, tracking quintessence is associated with a tracker orbit that originates from a tracker fixed point, T, on the $\tilde{\phi} = 0$ boundary, which in the present variables is given by

$$T : \quad (\tilde{\phi}, u, v) = (0, u_T, v_T) = (0, 1, 1) \sqrt{\frac{p}{2+p}}. \quad (53)$$

Notably T is a hyperbolic saddle with the ‘tracker orbit’ as its unstable manifold and $\tilde{\phi} = 0$ being its 2D stable manifold. This results in that an open set of nearby orbits is pushed toward the attractor orbit by the 2D invariant stable manifold boundary set $\tilde{\phi} = 0$, leading to that the tracker orbit acts as an ‘attractor orbit’ that describes the evolution of the open attracted set of tracking/shadowing orbits during their quintessence evolution, see [37] for details.

To find the parameters w_∞ , γ and β we first note that the tracker fixed point value for $u = u_T$ gives the past asymptotic tracker value for w_ϕ since

$$w_\infty = w_\phi|_T = u_T^2 - 1 = \frac{p}{2+p} - 1 = -\frac{2}{2+p}, \quad (54)$$

where w_∞ describes the single positive eigenvalue, given by $-3w_\infty = 6/(2+p)$. Next we proceed and make a series expansion in

$$T = T_0 e^{-3w_\infty N} \quad (55)$$

for the variables $(\tilde{\phi}, u, v)$. Since the governing equations (52) involve $\Gamma(\tilde{\phi})$ we need to use a truncated Taylor series of $\Gamma(\tilde{\phi})$ at $\tilde{\phi} = 0$:

$$\Gamma(\tilde{\phi}) \approx \Gamma^{(0)} + \Gamma^{(1)}\tilde{\phi} + \frac{1}{2}\Gamma^{(2)}\tilde{\phi}^2 + \dots, \quad \Gamma^{(n)} = \left. \frac{d^n \Gamma}{d\tilde{\phi}^n} \right|_{\tilde{\phi}=0}, \quad (56)$$

where $\Gamma^{(0)} = 1 + p^{-1}$.

To identify γ and β we solve for the coefficients for the series expanded variables $(\tilde{\phi}, u, v)$ by using the equations in (52), which when inserted into $w_\phi = u^2 - 1$ yields

$w_\phi \approx w_\infty [1 - (\gamma - 1)T(1 - \beta T)]$ with

$$\gamma = 1 - w_\infty^{-1}(1 - w_\infty^2)k, \quad (57a)$$

$$\beta = \frac{2w_\infty^2(3w_\infty - 1) + k(12w_\infty^4 - w_\infty^3 - 3w_\infty^2 + 2w_\infty - 1) + k^{(2)}}{w_\infty(12w_\infty^2 - 3w_\infty + 1)}, \quad (57b)$$

$$k = \frac{w_\infty - \frac{2}{3}\Gamma^{(1)}}{4w_\infty^2 - 2w_\infty + 1}, \quad (57c)$$

$$k^{(2)} = \frac{w_\infty\Gamma^{(2)}}{9(w_\infty + 1)k}, \quad (57d)$$

where we recall that $\Gamma^{(0)} = 1 + p^{-1}$, where $p > 0$ came from $V \propto \phi^{-p}$ when $\phi \rightarrow 0$, while $\Gamma^{(1)}$ and $\Gamma^{(2)}$ were defined in (56), $w_\infty = -2/(2 + p)$, and where $\tilde{\phi}$ was defined in (50), i.e., $\tilde{\phi} = (V_\phi/V)^{-2}$. In the expression for $k^{(2)}$ we assume that $k \neq 0$, since the special class of models with $k = 0$, i.e. $\Gamma^{(1)} = \frac{3}{2}w_\infty$, needs special treatment; note, however, that this class include models with $w_\phi = \text{constant} = w_\infty$, see [37] for details.¹⁴

Using (46) for tracking quintessence in connection with (30b) and (33) yields the following $w_\phi \approx [1/1]_{w_{\text{DE}}}(T)$ based *master tracking quintessence approximations*

$$w_\phi \approx [1/1]_{w_{\text{DE}}}(T) = - \left(1 - \frac{(\gamma - 1)T}{1 + \beta T} \right), \quad (58a)$$

$$\Omega_\phi \approx \frac{\Omega_{\phi 0}}{\Omega_{\text{m}0} e^{3w_\infty N} \left(\frac{1 + \beta T}{1 + \beta T_0} \right)^{\frac{\gamma - 1}{\beta}} + \Omega_{\phi 0}}, \quad (58b)$$

$$E_\phi^2 \approx \Omega_{\text{m}0} e^{-3N} + \Omega_{\phi 0} e^{-3(1 + w_\infty)N} \left(\frac{1 + \beta T_0}{1 + \beta T} \right)^{\frac{\gamma - 1}{\beta}}, \quad (58c)$$

where we recall that $T = T_0 \exp(-3w_\infty N)$, $T_0 = \Omega_{\phi 0}/(1 - \gamma\Omega_{\phi 0})$ while γ and β were given in the previous eq. (57). Setting $\beta = \gamma - 1$ in (58) in the above expressions yields the simpler, but less accurate, $w_\phi \approx [0/1]_{w_{\text{DE}}}(T)$ based tracking quintessence approximations. Again, to express our approximations in the redshift z , just use the simple relation $z = \exp(-N) - 1$. Section 5 provides a specific tracking quintessence example, the inverse power law potential $V \propto \phi^{-p}$, $p > 0$.

4 The Chevallier-Polarski-Linder parametrization

The so-called CPL parameters [27, 28] parametrize w_{DE} according to

$$w_{\text{DE}} = w_{\text{CPL}} := w_0 + w_a \left(1 - \frac{a}{a_0} \right), \quad (59)$$

which can be viewed as a truncated Taylor expansion in a/a_0 at the present time (i.e. at $a/a_0 = 1$), where a_0 is usually set to one, which when expressed in the redshift z

¹⁴Sahni and Starobinsky (2000) [50], equation (121), and Urena-Lopez and Matos (2000) [51], investigated models with the potential $V = V_0 \sinh^{-p}(\nu\phi)$ and showed that these models admit a special solution (which turns out to be the tracker orbit) for which w_ϕ is constant, i.e., they yield w_{CDM} spacetimes with $-1 < w_\phi = w_\infty = w < 0$.

takes the form $w_{\text{CPL}} = w_0 + w_a \left(\frac{z}{1+z}\right)$. Expressing the above equation in the e -fold time N yields

$$w_{\text{CPL}} = w_{\infty}^{\text{CPL}} - w_a e^N, \quad (60)$$

where $w_{\infty}^{\text{CPL}} := \lim_{N \rightarrow -\infty} w_{\text{CPL}}$, from which it follows that

$$w_{\infty}^{\text{CPL}} = w_0 + w_a. \quad (61)$$

Inserting (60) into (7) yields

$$f = e^{-3w_{\infty}^{\text{CPL}} N} \cdot e^{-3w_a(1-e^N)}, \quad (62)$$

which results in that (13) and (12) yield

$$\Omega_{\text{CPL}} = \frac{\Omega_{\text{DE0}}}{\Omega_{\text{m0}} e^{3w_{\infty}^{\text{CPL}} N} \cdot e^{3w_a(1-e^N)} + \Omega_{\text{DE0}}}, \quad (63a)$$

$$E_{\text{CPL}}^2 = \Omega_{\text{m0}} e^{-3N} + \Omega_{\text{DE0}} e^{-3(1+w_{\infty}^{\text{CPL}})N} \cdot e^{-3w_a(1-e^N)}. \quad (63b)$$

We note that the expressions in (63) do not have simple single series expansion since they mix the functions e^N and $e^{3w_{\infty}^{\text{CPL}} N}$, which is in contrast to our expressions that are based on the single function $e^{-3w_{\infty} N}$, as is w_{CDM} and Λ_{CDM} when $w_{\infty} = -1$.

Usually the CPL parameters are *cosmographically* determined by observations, but sometimes the $w_{\text{CPL}}(N)$ model with the parameters w_a and w_0 , where one of these parameters can be replaced with w_{∞}^{CPL} , is fitted to a *numerically* calculated solution of the quintessence field equations (due to that most scalar field potentials do not result in explicit solutions) with $w_{\phi}(N)$ at some time N_{fit} by requiring that

$$w'_{\text{CPL}}(N_{\text{fit}}) = -w_a e^{N_{\text{fit}}} = w'_{\phi}(N_{\text{fit}}), \quad (64a)$$

$$w_{\text{CPL}}(N_{\text{fit}}) = w_{\infty}^{\text{CPL}} - w_a e^{N_{\text{fit}}} = w_{\phi}(N_{\text{fit}}), \quad (64b)$$

from which we can obtain w_a , w_0 and w_{∞}^{CPL} at some fitting time N_{fit} as follows:

$$w_a = -e^{-N_{\text{fit}}} w'_{\phi}(N_{\text{fit}}), \quad (65a)$$

$$w_0 = w_{\phi}(N_{\text{fit}}) - w'_{\phi}(N_{\text{fit}})(1 - e^{-N_{\text{fit}}}), \quad (65b)$$

$$w_{\infty}^{\text{CPL}} = w_{\phi}(N_{\text{fit}}) - w'_{\phi}(N_{\text{fit}}), \quad (65c)$$

which if $N_{\text{fit}} = 0$ reduces to

$$w_a = -w'_{\phi}(0), \quad (66a)$$

$$w_0 = w_{\phi}(0), \quad (66b)$$

$$w_{\infty}^{\text{CPL}} = w_{\phi}(0) - w'_{\phi}(0). \quad (66c)$$

In stark contrast to earlier work we will now use our quintessence approximations to *analytically compute approximate observationally indistinguishable predictions* for the CPL parameters. Using the for thawing and tracking quintessence unifying equations in (30) for $w_{\phi}(N_{\text{fit}}) \approx w_{\text{DE}}(N_{\text{fit}})$ result in rather complicated expressions. For brevity we therefore use (26) where we recall that $T = T_0 \exp(-3w_{\infty} N)$, $T_0 = \Omega_{\phi 0} / (1 - \gamma \Omega_{\phi 0})$,

where we have replaced $\Omega_{\text{DE}0}$ with $\Omega_{\phi 0}$ since we now are concerned with quintessence. This leads to that the expression $w_\phi \approx [1/1]_{w_{\text{DE}}}(T)$ in (26b) results in

$$w_a = -3w_\infty e^{-N_{\text{fit}}} X, \quad (67a)$$

$$w_0 = w_\infty - [1 + 3w_\infty(1 - e^{-N_{\text{fit}}}) + \beta T_{\text{fit}}] X, \quad (67b)$$

$$w_\infty^{\text{CPL}} = w_\infty - (1 + 3w_\infty + \beta T_{\text{fit}})X, \quad (67c)$$

where X is defined as

$$X = \frac{w_\infty(\gamma - 1)T_{\text{fit}}}{(1 + \beta T_{\text{fit}})^2}, \quad (68)$$

where $T_{\text{fit}} = T_0 \exp(-3w_\infty N_{\text{fit}})$. As usual, the corresponding results for the $w_\phi \approx [0/1]_{w_{\text{DE}}}(T)$ are easily obtained from the above ones by replacing β with $\gamma - 1$. This leads to simpler expressions, but not sufficiently accurate for observational indistinguishability.

At the present time as fitting time, i.e. $N_{\text{fit}} = 0$, the equations in (67) yield

$$w_a \approx \frac{-3w_\infty^2(\gamma - 1)(1 - \gamma\Omega_{\phi 0})\Omega_{\phi 0}}{(1 + (\beta - \gamma)\Omega_{\phi 0})^2}, \quad (69a)$$

$$w_0 \approx w_\infty - \frac{w_\infty(\gamma - 1)\Omega_{\phi 0}}{1 + (\beta - \gamma)\Omega_{\phi 0}}, \quad (69b)$$

$$w_\infty^{\text{CPL}} = w_0 + w_a, \quad (69c)$$

which hence constitute our *analytic quintessence predictions* for the CPL parameters at the present time when our expressions for γ and β for quintessence are inserted. It follows that

$$\frac{w_a}{w_0 - w_\infty} \approx \frac{3w_\infty(1 - \gamma\Omega_{\phi 0})}{1 + (\beta - \gamma)\Omega_{\phi 0}} = 3w_\infty - \frac{3w_\infty\beta\Omega_{\phi 0}}{1 + (\beta - \gamma)\Omega_{\phi 0}}, \quad (69d)$$

for the $w_\phi \approx [1/1]_{w_{\text{DE}}}(T)$ case. As before, the expressions obtained from $w_\phi \approx [0/1]_{w_{\text{DE}}}(T)$ at $N_{\text{fit}} = 0$ are obtained by replacing β with $\gamma - 1$, where we note that $1 + (\beta - \gamma)\Omega_{\phi 0}$ then reduces to $1 - \Omega_{\phi 0} = \Omega_{\text{m}0}$. This leads to the following simple approximate estimate (which, unfortunately, is not at all as good as that in (69d))

$$\frac{w_a}{w_0 - w_\infty} \approx \frac{3w_\infty(1 - \gamma\Omega_{\phi 0})}{\Omega_{\text{m}0}} = 3w_\infty - 3w_\infty(\gamma - 1) \left(\frac{\Omega_{\phi 0}}{\Omega_{\text{m}0}} \right), \quad (70)$$

which thereby is linear in γ and equal to $3w_\infty$ for $w\text{CDM}$ since $\gamma = 1$ in this case. Thawing quintessence, for which $w_\infty = -1$, yields

$$\frac{w_a}{w_0 + 1} = -3 + 3(\gamma - 1) \left(\frac{\Omega_{\phi 0}}{\Omega_{\text{m}0}} \right) = -3 + \frac{8}{9} \left(\frac{\Omega_{\phi 0}}{\Omega_{\text{m}0}} \right) \epsilon_*, \quad (71)$$

due to (44). Thus if $\epsilon_* \approx 0$ then $w_a/(w_0 + 1) \approx -3$, however, viable thawing quintessence models typically admit a range of ϵ_* up to $\mathcal{O}(1)$, which results in a range for $w_a/(w_0 + 1) \in [-3, -1]$, cf. the discussion in [32], which requires the approximation in (69d) with $w_\infty = -1$ in order to achieve observational indistinguishability between a numerically computed thawing quintessence solution and our approximated one.

5 Numerical comparisons

In this section we calculate numerical relative errors for various types of approximations for quintessence, i.e.,

$$\left| \frac{\Delta F}{F} \right| = \left| \frac{F_{approx} - F_{num}}{F_{num}} \right|, \quad (72)$$

where we for brevity consider the relative errors for $w_\phi(z)$, $\Omega_m(z) = 1 - \Omega_\phi(z)$ and $E_\phi(z)$ (recall that $1 + z = \exp(-N)$). Apart from calculating the relative errors of our approximations for thawing and tracking quintessence, we will also calculate relative errors for approximations found in the literature, described in appendix A; in addition, we calculate the relative errors of the CPL approximation for quintessence, described in section 4, for which the CPL parameters w_0 and w_a must be calculated *numerically*. This in stark contrast to our purely *analytic* approximations which yield *predictions* for $w_\phi(z)$, $\Omega_m(z) = 1 - \Omega_\phi(z)$, $E_\phi(z)$ and the CPL parameters w_0 and w_a . Furthermore, in order to illustrate that our most accurate approximations eliminate the need for numerical CPL quintessence calculations, we compute

$$\begin{aligned} \Delta(F_{[0/1]}) &= \left\| \left| \frac{F_{CPL} - F_{num}}{F_{num}} \right| - \left| \frac{F_{CPL} - F_{[0/1]}}{F_{[0/1]}} \right| \right\|, \\ \Delta(F_{[1/1]}) &= \left\| \left| \frac{F_{CPL} - F_{num}}{F_{num}} \right| - \left| \frac{F_{CPL} - F_{[1/1]}}{F_{[1/1]}} \right| \right\|, \end{aligned} \quad (73)$$

where $F = w_\phi(z)$, $F = \Omega_m(z) = 1 - \Omega_\phi(z)$ and $F = E_\phi(z)$, while the subscripts $_{[0/1]}$ and $_{[1/1]}$ refer to our two approximations.

We cannot of course test all possible scalar field potentials, but we have done so with several potentials and obtained similar results. For brevity we will here only present the results for two specific scalar field potentials, one illustrating relative approximation errors for thawing quintessence and one for tracking quintessence.

Thawing quintessence

For thawing quintessence we will consider a currently popular model, the quintessential α -attractor inflation model introduced in [52] and further explored in [53], [54] and [38], referred to as Exp-model I in [53], [54] and as the EC potential model in [38], given by

$$V = V_- e^{-\nu(1+\bar{\phi})}, \quad \bar{\phi} = \tanh\left(\frac{\phi}{\sqrt{6\alpha}}\right), \quad (74)$$

which results in

$$\lambda = \frac{\nu}{\sqrt{6\alpha}} (1 - \bar{\phi}^2), \quad \lambda_{,\phi} = -\left(\frac{\nu}{3\alpha}\right) \bar{\phi} (1 - \bar{\phi}^2). \quad (75)$$

As a consequence (42) yields

$$\epsilon_* = \frac{\nu^2}{12\alpha} (1 - \bar{\phi}_*^2)^2, \quad \eta_* = \frac{\nu}{6\alpha} (1 - \bar{\phi}_*^2) [\nu (1 - \bar{\phi}_*^2) + 2\bar{\phi}_*], \quad (76)$$

where $\bar{\phi}_*(\phi_*)$, $\phi_* \in [-\infty, \infty]$, represents a freezing value of ϕ during the matter dominated epoch for the 1-parameter set of attractor thawing solutions with model parameters α and ν (V_- represents an overall scaling parameter and do not appear in the dimensionless quantities $w_\phi(z)$, $\Omega_m(z) = 1 - \Omega_\phi(z)$ and $E_\phi(z)$).

The parameters γ and β follow trivially from (47) and are given by

$$\gamma = 1 + \frac{2\nu^2}{81\alpha} (1 - \bar{\phi}_*^2)^2, \quad \beta = \frac{3}{5} + \frac{4\nu}{405\alpha} (1 - \bar{\phi}_*^2) [2\nu (1 - \bar{\phi}_*^2) + 9\bar{\phi}_*], \quad (77)$$

where (47) also yields our $w_\phi \approx [1/1]_{w_{\text{DE}}}(T(z))$ based approximations while setting $\beta = \gamma - 1$ into (47) first and then the above expression for γ into the resulting expression yields our simpler but less accurate $w_\phi \approx [0/1]_{w_{\text{DE}}}(T(z))$ based approximations.

To compare with numerics we have to specify the model parameters α and ν . We follow [38] and set them to $(\alpha, \nu) = (\frac{7}{3}, 128)$. We also need to specify which one of the 1-parameter set of thawing quintessence attractor solutions, parametrized by ϕ_* , we consider. These models were discussed in [38] in the context quintessential inflation, where inflationary considerations determined the overall energy scale V_- , see [53] and [54]. The inclusion of radiation yielded an integral, which resulted in that only one of the thawing quintessence attractor solutions in the 1-parameter set characterized by ϕ_* was compatible with the chosen values of V_- , H_0 , $\Omega_{\gamma 0}$ and Ω_{m0} . This solution was found by varying the frozen scalar field value, ϕ_* , at the line of fixed points from which the thawing quintessence attractor solutions originated, which resulted in $\phi_* = 9.594$. In the present case where we neglect radiation the integral does not exist and then H_0 and $\Omega_{\phi 0} = 0.68$ do not impose any restrictions on ϕ_* at the line of fixed points $(\phi, \Sigma_-, \Omega_\phi) = (\phi_*, 0, 0)$ from which the thawing quintessence attractor solutions originate. However, due to that radiation is negligible when quintessence affects the evolution, the present approximations for e.g. $w_\phi(z)$, $\Omega_\phi(z)$, $E_\phi(z)$ are excellent also when radiation is included as in [38]. For this reason, although not necessary, we choose $\phi_* = 9.594$ in order to make contact with our previous work in [38]. Inserting $\phi_* = 9.594$ and $(\alpha, \nu) = (\frac{7}{3}, 128)$ into (74) and (77) result in

$$(\gamma, \beta) = (1.095, 0.789), \quad (78)$$

thereby making the approximation numerically explicit. To obtain the relative errors we numerically integrate the dynamical system (37) and the decoupled equation for $E_\phi = H_\phi/H_0$,

$$E'_\phi = -\frac{3}{2}(1 + w_{\text{tot}}) E_\phi = -\frac{3}{2}(1 + w_\phi \Omega_\phi) E_\phi = -\frac{3}{2}(1 - \Omega_\phi + 2\Sigma_\phi^2) E_\phi, \quad (79)$$

where we have used (15), (16) and (36). We then change from e -fold time N to the redshift z via $z = \exp(-N) - 1$.

The relative errors of $w_\phi(z)$, $\Omega_m(z) = 1 - \Omega_\phi(z)$ and $E_\phi(z)$ for several approximations are depicted in Figure 1. These include analytic approximations such as our $w_\phi \approx [0/1]_{w_{\text{DE}}}(T(z))$ and $w_\phi \approx [1/1]_{w_{\text{DE}}}(T(z))$ based approximations, as well as the approximations by Scherrer and Sen [55] and Chiba [56], given by the equations (88) and (94), respectively, in appendix A. In addition we give the CPL approximation based on the numerically calculated values for w_0 and w_a at $z = 0$, which thereby, of course, results in no error for w_ϕ at $z = 0$.

As can be seen, the earlier analytic approximations by Scherrer and Sen [55] and Chiba [56]¹⁵ and the more simple and consistent $w_\phi \approx [0/1]_{w_{\text{DE}}}(T(z))$ approximant based approximations have similar relative errors for the physical observables Ω_m and E_ϕ , with respective $\sim 3\%$ and $\sim 1.5\%$ maxima, while the $w_\phi \approx [1/1]_{w_{\text{DE}}}(T(z))$ approximant yields a maximum relative error of $\sim 0.1\%$ for Ω_m and an even smaller error for E_ϕ , making this approximation observationally indistinguishable from numerical results. Not even the numerically based CPL approximation, with no predictive power at $z = 0$, is as good as our analytic $w_\phi \approx [1/1]_{w_{\text{DE}}}(T(z))$ based approximations.

Note that if we instead of using $T_0 = \Omega_{\phi 0}/(1 - \gamma\Omega_{\phi 0})$ use the numerically computed $w_0 = w_{\phi 0}$ in T_0 as described in eq. (27) we get even more accurate results than our previous approximations and the CPL based approximations, but then this results in that the *purely analytic predictions* of our quintessence approximations are lost.

Finally, note that changing ϕ_* so that $\lambda_* = \lambda(\phi_*)$ decreases also decreases the errors, which is due to slower rolling of the scalar field. Note also that the errors of all approximations decrease as z increases, which should not come as a surprise since increasing z entails increased matter domination. Investigations of several other scalar field potentials yield similar results.

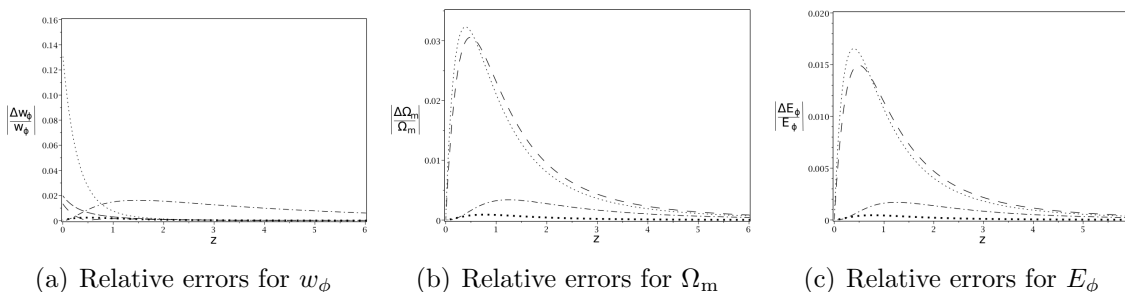


Figure 1: *Thawing quintessence*: Relative errors $|\Delta F/F|$ for $w_\phi(z)$, $\Omega_m(z)$, $E_\phi(z)$. The dotted curves depict the relative errors of the new $w_\phi \approx [0/1]_{w_{\text{DE}}}(T(z))$ based approximations, i.e., (47) with $\beta = \gamma - 1$, while the thick dotted curves represent the relative errors of the $w_\phi \approx [1/1]_{w_{\text{DE}}}(T(z))$ based approximations (47). The dash-dotted curves correspond to the CPL based approximations with the numerically determined values $(w_0, w_a) = (-0.9186, -0.0871)$. In Figure (a) the dashed curve is the approximation by Scherrer and Sen [55] given in eq. (88), while the space-dashed curve is the approximation obtained by Chiba [56], see eq. (94). In Fig. (b) and (c) the dashed curves correspond to the Λ CDM solution given in (19), which is the basis for the approximations of both Scherrer and Sen [55] and Chiba [56].

Figure 2 contains the differences $\Delta(w_\phi(z))$, $\Delta(\Omega_m(z))$ and $\Delta(E_\phi(z))$ between relative CPL errors and the relative difference between CPL and our approximations, as described in eq. (73). The simple $w_\phi \approx [0/1]_{w_{\text{DE}}}(T(z))$ approximant based approximations yields order of estimate descriptions of the CPL approximations but is not sufficiently good to make numerical calculations unnecessary. On the other hand, our

¹⁵Here we have treated these approximations in the same way as our approximations, i.e. as analytic predictive approximations. This is not how they were dealt with in the original references. There numerical calculations picked out a particular solution in the 1-parameter set of thawing solutions, which results in less errors at the price of losing predictive power.

analytic $w_\phi \approx [1/1]_{w_{\text{DE}}}(T(z))$ approximant based approximations are virtually indistinguishable from numerical results, again illustrating that this approximation is so good so that it makes numerical calculations irrelevant.

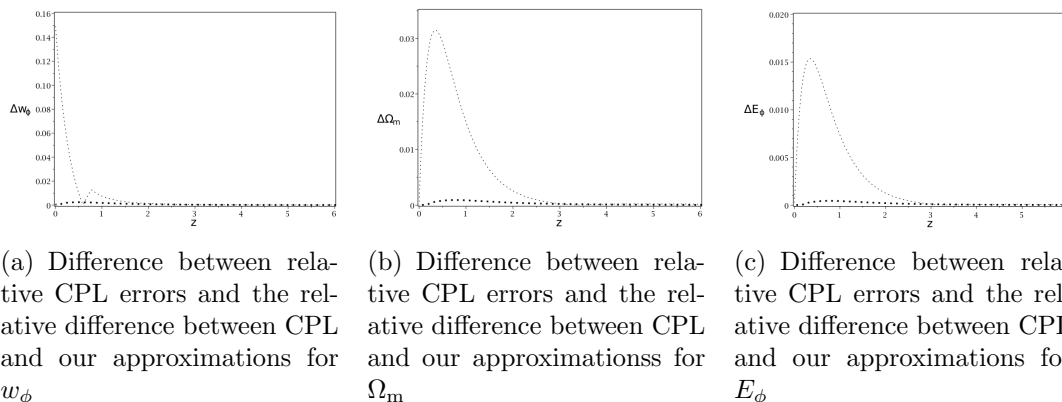


Figure 2: *Thawing quintessence*: Difference between relative CPL errors and the relative difference between CPL and our approximations based on $w_\phi \approx [0/1]_{w_{\text{DE}}}(T(z))$ (dotted curves) and $w_\phi \approx [1/1]_{w_{\text{DE}}}(T(z))$ (thick dotted curves), as described in equations (73) for $\Delta(w_\phi(z))$, $\Delta(\Omega_m(z))$, $\Delta(E_\phi(z))$, emphasizing that the analytic $w_\phi \approx [1/1]_{w_{\text{DE}}}(T(z))$ based approximations are observationally indistinguishable from numerically based CPL approximations, making such numerical explorations unnecessary.

We finally note that our numerical calculations yield $(w_0, w_a) \approx (-0.9186, -0.0871)$, and hence $w_\infty^{\text{CPL}} \approx -1.0057$ and $\frac{w_a}{w_0+1} \approx -1.0700$. Using our $w_\phi \approx [1/1]_{w_{\text{DE}}}(T(z))$ approximant, which yields equation (69), where we recall that $w_\infty = -1$ for thawing quintessence, results in $(w_0, w_a) \approx (-0.9183, -0.0791)$ and hence $w_\infty^{\text{CPL}} \approx -0.9974$ and $\frac{w_a}{w_0+1} \approx -0.9682$, which illustrates how good this approximation is.

Tracking quintessence

As our example for tracking quintessence we choose the inverse power law potential, for which

$$V = V_0 \phi^{-p}, \quad \lambda = \frac{p}{\phi}, \quad \Gamma = 1 + \frac{1}{p} = \text{constant}. \quad (80)$$

Thus the derivatives of Γ are zero and hence $\Gamma^{(1)} = 0$ and $\Gamma^{(2)} = 0$ in (57), while, as for all the present tracking quintessence models,

$$w_\infty = -\frac{2}{2+p}, \quad (81)$$

where we will use w_∞ rather than $p = -2(1+w_\infty)/w_\infty$ since this leads to somewhat more succinct expressions. The expressions for γ and β for this case follows straight-

forwardly from (57) and can be written as

$$\gamma = 1 - \frac{1 - w_\infty^2}{4w_\infty^2 - 2w_\infty + 1}, \quad (82a)$$

$$\beta = \frac{36w_\infty^4 - 21w_\infty^3 + 7w_\infty^2 - 1}{(4w_\infty^2 - 2w_\infty + 1)(12w_\infty^2 - 3w_\infty + 1)}. \quad (82b)$$

which for $p = 1$ yields $w_\infty = -2/3$ and $(\gamma, \beta) \approx (0.86486, 0.45081)$, while, e.g., $p = 0.1$ results in $w_\infty = -20/21 \approx -0.95238$ and $(\gamma, \beta) \approx (0.98577, 0.55145)$. Inserting these results into (58) yields our tracking quintessence approximations (as before, setting first $\beta = \gamma - 1$ yields our $w_\phi \approx [0/1]_{w_{\text{DE}}}(T(z))$ based approximations). To make numerical comparisons with our approximations we choose the historically important case $p = 1$ described above, though this value might be too large to constitute an observationally viable model.

For numerical calculations we use the system (52) and the value $\Omega_{\phi_0} = 0.68$, which form a surface in the $(\tilde{\phi}, u, v)$ state space that intersects the tracker orbit at a point found numerically, thus identifying where $N = 0$, and where the numerical calculations also give us $w_\phi = u^2 - 1$, $\Omega_m = 1 - \Omega_\phi = 1 - 3\tilde{\phi}v^2$, while E_ϕ is found numerically by integrating¹⁶

$$E'_\phi = -\frac{3}{2}(1 + w_{\text{tot}})E_\phi = -\frac{3}{2}(1 + w_\phi\Omega_\phi)E_\phi = -\frac{3}{2}\left[1 + 3\tilde{\phi}v^2(u^2 - 1)\right]E_\phi. \quad (83)$$

Figure 3 depicts the relative errors of our approximations and the Chiba approximations [57] for Ω_m and E_ϕ . Notably the Chiba approximations are rather poor, even when compared to the $w_\phi \approx [0/1]_{w_{\text{DE}}}(T(z))$ based approximation, which also have relative errors of several %, while the $w_\phi \approx [1/1]_{w_{\text{DE}}}(T(z))$ based approximations again are excellent with, e.g., a relative error of $\sim 0.1\%$ for E_ϕ . This is also the case for the CPL approximation, but in contrast to our purely analytic approximations the parameters w_0 and w_a were fitted numerically at the present time. If we instead of using Ω_{ϕ_0} in T_0 use the numerically computed $w_0 = w_{\phi_0}$ in T_0 as described in eq. (27) we get even more accurate results than our previous approximation and the CPL approximation, but then this results in that the analytic predictions of our approximations are lost.

Finally, note that decreasing p to obtain observationally viable models yields even better results since the maximal errors for the $w_\phi \approx [1/1]_{w_{\text{DE}}}(T(z))$ based approximations are roughly proportional to p , e.g. $p = 0.1$ yields a maximal relative error $\sim 0.01\%$ for E_ϕ . Thus, again the $w_\phi \approx [1/1]_{w_{\text{DE}}}(T)$ based approximations are observationally indistinguishable from numerical results.

We then note that for $p = 1$, our numerical calculations yield $(w_0, w_a) \approx (-0.7581, 0.1080)$, and hence $w_\infty^{\text{CPL}} \approx -0.6501$ and $\frac{w_a}{w_0 - w_\infty} \approx -1.1812$, where we recall $w_\infty = -2/3 \approx -0.6667$. The $w_\phi \approx [1, 1]_{w_{\text{DE}}}$ approximation yields $(w_0, w_a) \approx (-0.7519, 0.0978)$, and hence $\frac{w_a}{w_0 - w_\infty} \approx -1.1474$. Decreasing p yields even better results.

Figure 4 contains the differences $\Delta(w_\phi(z))$, $\Delta(\Omega_m(z))$ and $\Delta(E_\phi(z))$ between relative CPL errors and the relative difference between CPL and our approximations, as described in eq. (73). Again, the simple $w_\phi \approx [0/1]_{w_{\text{DE}}}(T(z))$ approximant based approximations yields order of estimate descriptions of the CPL approximations but not good

¹⁶The present model, like all scalar field models, also admits a 1-parameter set of thawing quintessence attractor solutions in the state space, see [37], which we for brevity do not discuss.

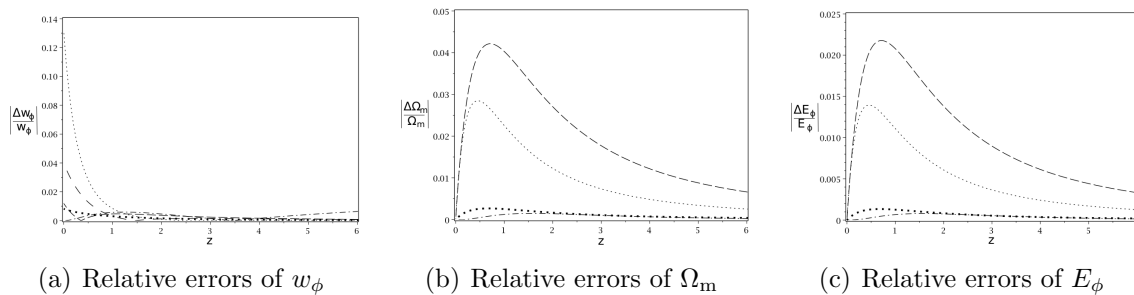


Figure 3: *Tracking quintessence*: Relative errors $|\Delta F/F|$ for $w_\phi(z)$, $\Omega_m(z) = 1 - \Omega_\phi(z)$, $E_\phi(z)$. The dotted curves depict the relative errors for the $w_\phi \approx [0/1]_{w_{\text{DE}}}(T(z))$ based approximations following from (58), while the thick dotted curves represent the relative errors for the $w_\phi \approx [1/1]_{w_{\text{DE}}}(T(z))$ based approximations in (58). The dashed-dotted curves correspond to the CPL based approximations with, at the present time, numerically calculated values $(w_0, w_a) = (-0.7581, 0.1080)$. In Figure (a) the space-dashed and dashed curves describe the Chiba approximation [57], given in (97), truncated at 1st and 2nd order in Ω_ϕ , respectively. In Fig. (b) and (c) the dashed curves depict the w CDM solution given in (19), which form the basis for the Chiba approximations.

enough for a detailed description; on the other hand, our analytic $w_\phi \approx [1/1]_{w_{\text{DE}}}(T(z))$ approximant based approximations are very close to the numerical results, again illustrating that our best approximations are so good so that they make numerical calculations irrelevant.

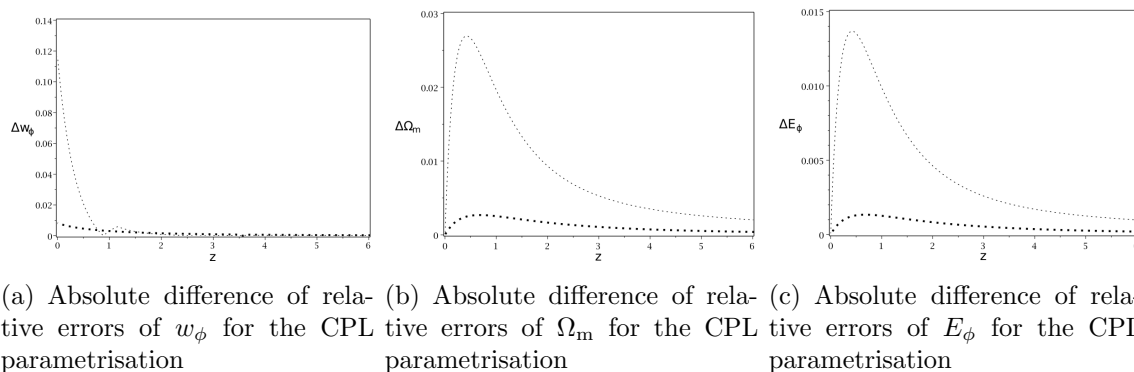


Figure 4: *Tracking quintessence*: Absolute difference between relative errors, as described in equations (73), for the CPL parametrisation relative to the numerical solution and the $w_\phi \approx [0/1]_{w_{\text{DE}}}(T(z))$ (dotted curves) and $w_\phi \approx [1/1]_{w_{\text{DE}}}$ (thick dotted curves) based approximations for $w_\phi(z)$, $\Omega_m(z)$, $E_\phi(z)$, emphasizing that the analytic $w_\phi \approx [1/1]_{w_{\text{DE}}}(T(z))$ based approximations are observationally indistinguishable from numerical calculations, making the latter unnecessary.

6 Discussion

In this paper we have derived simple and accurate approximations for thawing and tracking quintessence. This was accomplished by identifying that thawing and tracking quintessence are associated with ‘attractor solutions’ for which $\lim_{N \rightarrow -\infty} \Omega_\phi = 0$ (and hence $\lim_{N \rightarrow -\infty} \Omega_m = 1$) and $\lim_{N \rightarrow -\infty} w_\phi = w_\infty$, where $w_\infty = -1$ for thawing quintessence while $-1 < w_\infty < 0$ for tracking quintessence. These asymptotic properties served as motivation for situating the derivation of the quintessence approximations in a unifying DE context. It was shown that the conditions $\lim_{N \rightarrow -\infty} \Omega_\phi = 0$ and $\lim_{N \rightarrow -\infty} w_\phi = w_\infty \in [-1, 0)$ naturally resulted in series expansions in $T = T_0 \exp(-3w_\infty N)$. However, since our goal was to obtain accurate approximations during the whole time period between matter dominance, i.e. when $\Omega_\phi \approx 0$ and $\Omega_m \approx 1$, and the present time for thawing and tracking quintessence we used Padé approximants where the $[1/1]_{\Omega_{\text{DE}}}$ Padé approximant for Ω_{DE} was used to relate the approximations to the present time initial value $\Omega_{\text{DE}0}$, or, equivalently, $\Omega_{\text{m}0} = \rho_{\text{m}0}/3H_0^2$.

After the unifying DE section we specialized to thawing and tracking quintessence by deriving two dynamical systems adapted to the two different types of quintessence. This allowed us to insert the DE series expansions into these two dynamical systems and solve for γ and β , which then via the $[0/1]_{w_{\text{DE}}}(T(z))$ and $[1/1]_{w_{\text{DE}}}(T(z))$ based DE expressions, and changing $\Omega_{\text{DE}0}$ to $\Omega_{\phi 0}$, yield corresponding quintessence approximations for $\Omega_\phi(z)$ and $E(z) = H(z)/H_0$. Note that for a given potential, the parameters in our approximations precisely correspond to the dimensionless parameters in the potential, since they are easily analytically computed from the potential by taking scalar field derivatives; thus, no extra parameters occur in our approximate expressions, although note that thawing quintessence, which exists for *all* scalar field potentials, also involves a 1-parameter set of solutions described by the freezing value ϕ_* during the matter dominated epoch. We also showed numerically that the $w_\phi(z) \approx [1/1]_{w_{\text{DE}}}(T(z))$ based approximations are an order of magnitude more accurate than any previous analytic approximations in the literature, making numerical calculations for thawing and tracking quintessence unnecessary. Moreover, we showed how one can *analytically* compute the CPL parameters, again with an accuracy that eliminates the need for numerical calculations of these parameters.

In this paper we have followed the majority of work in this area by focussing on generating results from w_ϕ , but there are many other possibilities, as well as further developments and applications, where we describe some in the following list:

- Instead of using w_ϕ as the starting point, one can use other variables. For example, as pointed out in footnote 7, our series expansions also give rise to a series expansion in T for E_{DE}^2 and thereby also for E_{DE} and E_ϕ . This expansion can subsequently be used to obtain various Padé approximants, which can then serve as the starting point for calculating other quantities. Or one can derive series expansions for one of the distance measures and use this for constructing Padé approximants, from which other variables and observables can be derived.
- We have here neglected radiation, which, however, can be included in several different ways; one can e.g. use the fixed points on the radiation boundary as the starting point instead of the fixed points on the matter boundary when it

comes to quintessence, as was done in [38]. Or one can simply add radiation, $\rho_\gamma = \rho_{\gamma 0} \exp(-4N) = 3H_0^2 \Omega_{\gamma 0} \exp(-4N)$, to ρ , i.e. $\rho = \rho_\gamma + \rho_m + \rho_{\text{DE}}$, and keep the present w_{DE} expressions, since radiation has a negligible influence on quintessence evolution, and, e.g., use that $3H^2 = \rho$.

- For some purposes there might be of interest to obtain an expression for how the scalar field changes during thawing quintessence from the past freezing value ϕ_* during the matter dominant epoch to some arbitrary e -fold time N . This can be done in several ways, but constructing the $[1, 1]_{\phi'}$ Padé approximant on the right hand side of ϕ' in (41b), i.e. $\sqrt{3(\gamma - 1)} T / (1 + \sigma T)$ where $\sigma = \frac{4}{5} \left(1 + \frac{\eta_*}{6}\right)$, and then integrating from $-\infty$ to N yields an excellent approximation¹⁷ given by

$$\phi = \phi_* + \sqrt{\frac{1}{3}(\gamma - 1)} \left(\frac{1}{\sigma}\right) \ln \left(1 + \frac{\sigma \Omega_{\phi 0}}{(1 - \gamma \Omega_{\phi 0}) e^{-3N}}\right). \quad (84)$$

- One can use other dynamical systems variables than the present ones to obtain somewhat different results. For example, we could have used the variables in [37] to deal with tracking quintessence, which would have been useful for the hyperbolic potentials that in addition to the inverse power law potential was dealt with in that paper.¹⁸ However, to improve convergence one should then replace the scalar field variable $\bar{\varphi}$ in [37] with $\tilde{\varphi} = \bar{\varphi}^2$.
- In the spirit of CPL, it is possible to improve our quintessence approximations even further by viewing γ and β as numerically determined parameters. This, however, means that one (similarly to CPL) would only do curve fitting, which implies less theoretical content and predictive power.
- We have here focussed on obtaining thawing and tracking quintessence approximations situated in a broader unifying DE context for spatially homogeneous, isotropic and flat spacetimes. A natural next step is to use these approximations in order to interpret and assess the rapidly growing set of increasingly precise observational data. In particular, the present results, or variations thereof, can serve as input in cosmological perturbation theory to bring the results closer to a wide set of observations.
- We finally note that the present approach and variations thereof can easily be applied to other models and theories, especially for those admitting an Einstein frame, although this usually adds parameters that diminish predictive power.

Acknowledgments

A. A. is supported by FCT/Portugal through CAMGSD, IST-ID, projects UIDB/04459/2020 and UIDP/04459/2020, and by the H2020-MSCA-2022-SE project EinsteinWaves, GA

¹⁷It is, e.g., a better approximation than that of Raveri *et al.* [58] given in equation (90) in appendix A.

¹⁸This would had come with the price that Γ would not have appeared explicitly in the results for γ and β due to the different regularization of λ .

No. 101131233. A.A. would also like to thank the CMA-UBI in Covilhã for kind hospitality. C. U. would like to thank the CAMGSD, Instituto Superior Técnico in Lisbon for kind hospitality.

A Quintessence approximations and comparisons

In this appendix we review the most prominent quintessence approximations in the literature, including some simplified derivations and extensions; moreover, we will present them in a more unified and concise manner than their original form. We begin with thawing quintessence.

A.1 Thawing quintessence

Let us first derive an approximation introduced by Sherrer and Sen (2008) in [55] and further explored by e.g. Agrawal *et al.* [59] and Raveri *et al.* [58]. Instead of using the state vector $(\phi, \Sigma_\phi, \Omega_\phi)$ we construct a dynamical system closely connected with $\tilde{\phi}, u, v$ based on the state vector (ϕ, u, ω) where¹⁹

$$u = \Sigma_\phi \sqrt{\frac{2}{\Omega_\phi}} = \frac{\phi'}{\sqrt{3\Omega_\phi}}, \quad \omega = \sqrt{\Omega_\phi}, \quad (85)$$

which due to (37) yields the dynamical system

$$\phi' = \sqrt{3}u\omega, \quad (86a)$$

$$u' = \frac{1}{2}(2 - u^2)[\sqrt{3}\lambda(\phi)\omega - 3u], \quad (86b)$$

$$\omega' = \frac{3}{2}(1 - u^2)\omega(1 - \omega^2). \quad (86c)$$

Next ϕ is assumed to take a frozen constant value $\phi = \phi_*$ while the two last equations in (86) are linearized in *u only*, which results in the following equations for u and ω :

$$u' \approx -3u + \sqrt{3}\lambda_*\omega, \quad (87a)$$

$$\omega' \approx \frac{3}{2}\omega(1 - \omega^2), \quad (87b)$$

where $\lambda_* = \lambda(\phi_*)$. The second equation, which corresponds to $\Omega'_\phi \approx 3\Omega_\phi(1 - \Omega_\phi)$ and hence $[\ln\{\Omega_\phi/(1 - \Omega_\phi)\}]' = [\ln(\Omega_\phi/\Omega_m)]' = [\ln(\rho_\phi/\rho_m)]' \approx 3$, where $\rho_m = \rho_{m,0} \exp(-3N)$ yields $\rho_\phi \propto \text{constant}$ and thereby the Λ CDM expression for $\omega(N)$. Inserting this solution into (87a) and integrating gives $u(N)$, from which $w_\phi = u^2 - 1$ follows; deparameterizing the solution results in $u(\omega)$ and thereby $w_\phi(\omega)$; alternatively, solve directly

¹⁹The variable u was introduced in [36] while the variable v in that paper is just $v = \omega/\sqrt{3}$.

$$du/d\omega = u'/\omega' \approx -\frac{2u}{\omega(1-\omega^2)} + \frac{2\lambda_*}{\sqrt{3}(1-\omega^2)}:$$

$$\begin{aligned} 1 + w_\phi &= \frac{\lambda_*^2}{3} [\omega^{-1} - (\omega^{-2} - 1) \tanh^{-1}(\omega)]^2 \\ &= \frac{\lambda_*^2}{3} [\Omega_\phi^{-1/2} - (\Omega_\phi^{-1} - 1) \tanh^{-1}(\Omega_\phi^{1/2})]^2, \end{aligned} \quad (88a)$$

$$\Omega_\phi = [1 + (\Omega_{\phi 0}^{-1} - 1) e^{-3N}]^{-1}, \quad (88b)$$

where the last expression coincides with that of Λ CDM when identifying Ω_ϕ with Ω_Λ (this approximation thereby does not give thawing corrections to the line element since it is just the Λ CDM line element); the above expressions summarize eqs. (23), (25) and (26) in Scherrer and Sen [55]. Taken together with eq. (86a) and $u^2 = 1 + w_\phi$ this results in

$$\phi' = \lambda_* [1 - (\omega^{-1} - \omega) \tanh^{-1}(\omega)] = \lambda_* [1 - (\Omega_\phi^{-1/2} - \Omega_\phi^{1/2}) \tanh^{-1}(\Omega_\phi^{1/2})], \quad (89)$$

where inserting (88b) yields $\phi'(N)$. This expression agrees with eq. (15) in Agrawal *et al.* [59] for the exponential potential for which λ is a constant. Integration, with the condition that $\phi = \phi_*$ when $N \rightarrow -\infty$ and $\Omega_\phi \rightarrow 0$ (using $\phi' = \Omega'_\phi d\phi/d\Omega_\phi$ and $\Omega'_\phi \approx 3\Omega_\phi(1 - \Omega_\phi)$), results in

$$\phi \approx \phi_* + \frac{2\lambda_*}{3} [\Omega_\phi^{-1/2} \tanh^{-1}(\Omega_\phi^{1/2}) - 1], \quad (90)$$

where $\phi(N)$ is obtained by inserting (88b). This approximation coincides with eq. (8) in Raveri *et al.* [58].

Other types of thawing quintessence approximations in the literature are based on series expansions of $V(\phi)$ at some ϕ_* , and thus also of $\lambda(\phi)$ when the latter is regular at ϕ_* . An example of this were given by Cahn *et al.* (2008) [60] who gave approximate expressions for ϕ' (replacing $\dot{\phi}$ with ϕ' in their eq. (15)) and ϕ , although note that ϕ_* is missing in their eq. (16), thus hiding that you typically are interested in a domain of ϕ_* . These expressions correspond to the present second order expressions in eqs. (41a) and (41b), whose accuracy we subsequently improved by taking Padé approximants.

Based on earlier results by Dutta and Scherrer (2008) [61], Chiba (2009) [56] Taylor expanded the potential to second order in $\phi - \phi_*$. By a sequence of *ad hoc* approximations in the proper time t the author derived a series of results (see p. 083517-4 in [56]), which can be extended to also include ϕ' and w_{tot} , more simply expressed in $\omega = \sqrt{\Omega_\phi}$ as follows:

$$\phi = \phi_* + \frac{2\lambda_*}{3} \left(\frac{(1 - \omega^2)^{\frac{1}{2}(1-K)} [(1 + \omega)^K - (1 - \omega)^K] - 2K\omega}{K\omega(K^2 - 1)} \right), \quad (91a)$$

$$\phi' = \lambda_* \frac{(1 - \omega^2)^{\frac{1}{2}(1-K)} [(1 + K\omega)(1 - \omega)^K - (1 - K\omega)(1 + \omega)^K]}{K\omega(K^2 - 1)}, \quad (91b)$$

$$1 + w_\phi = \frac{\lambda_*^2}{3} (1 - \omega^2)^{1-K} \left[\frac{(1 + K\omega)(1 - \omega)^K - (1 - K\omega)(1 + \omega)^K}{K\omega^2(K^2 - 1)} \right]^2, \quad (91c)$$

$$w_{\text{tot}} = w_\phi \omega^2, \quad (91d)$$

where

$$K = \sqrt{1 - \frac{4}{3}\eta_*}, \quad (92)$$

while $\omega = \sqrt{\Omega_\phi}$ is given by its Λ CDM expression

$$\omega = (1 + (\Omega_{\phi 0}^{-1} - 1)e^{-3N})^{-1/2}. \quad (93)$$

The right hand side for ϕ' was obtained by using $\phi' = \frac{d\phi}{d\omega}\omega'$ and the Λ CDM relation $\omega' = \frac{3}{2}(1 - \omega^2)\omega$. Taking the limit $K \rightarrow 1$ of equations (91a) and (91b), which corresponds to neglecting the second order Taylor expansion term of the potential, i.e. setting $V_{,\phi\phi}(\phi_*) = 0$, leads to an indeterminacy that can be solved by L'Hôpital's rule. In [56] the author also showed how to convert the expression for w_ϕ to the case when $K^2 < 0$, which resulted in the approximation

$$1 + w_\phi = \frac{4}{3}\lambda_*^2(1 - \omega^2) \left[\frac{\tilde{K}\omega \cos\left(\tilde{K} \sinh^{-1}\left(\frac{\omega}{\sqrt{1-\omega^2}}\right)\right) - \sin\left(\tilde{K} \sinh^{-1}\left(\frac{\omega}{\sqrt{1-\omega^2}}\right)\right)}{\tilde{K}\omega^2(1 + \tilde{K}^2)} \right]^2, \quad (94)$$

where

$$\tilde{K} = \sqrt{\frac{4}{3}\eta_* - 1}. \quad (95)$$

In addition, Chiba [56] discussed the approximation given by Crittenden *et al.* (2007) [62].

A.2 Tracking quintessence

Here we consider the tracking quintessence approximations given by Chiba (2010) [57], which in turn relied on earlier work by Watson and Scherrer (2003) [63], for the case $\Gamma = \text{constant}$, and, in particular, $\Gamma = \text{constant} > 1$, which yields the inverse power law potential. This work is based on a linearized equation for a perturbation of w_ϕ with respect to its asymptotic value w_∞ . To obtain an improved approximation for the *linearized solution* for w_ϕ Chiba [57] considered a series expansion in $e^{-3w_\infty N}$, when expressed in e -fold time and the present notation. This is the same series expansion quantity as in the present paper, but in contrast to Chiba [57] we used it to produce approximations for the full *non-linear* equations; thus, the expansions in the present work coincide with those in [63] and [57] for the quantities that have been computed in those two references up to first order but not for higher orders since Chiba [57] only deals with the linearized equation for w_ϕ . Moreover, there is translation freedom in N . In the present work this freedom was fixed by the $[1/1]_{\Omega_\phi}$ Padé approximant for Ω_ϕ , which resulted in an expansion in $T = \Omega_{\phi 0} e^{-3w_\infty N} / (1 - \gamma \Omega_{\phi 0})$; Chiba [57] on the other hand fixed this freedom by, in effect, setting $w_\phi = w_\infty$, to obtain the following approximation for Ω_ϕ :

$$\Omega_\phi \approx \frac{\tilde{T}}{1 + \tilde{T}} = \frac{\Omega_{\phi 0}}{\Omega_{\phi 0} + (1 - \Omega_{\phi 0})e^{3w_\infty N}}, \quad \tilde{T} = \left(\frac{\Omega_{\phi 0}}{1 - \Omega_{\phi 0}} \right) e^{-3w_\infty N}, \quad (96)$$

which corresponds to w CDM, while the series expansion in \tilde{T} for the linearized equation for w_ϕ resulted in

$$w_\phi = w_\infty + w_\infty(1 - w_\infty^2) \sum_{n=1}^{\infty} \left(\frac{(-1)^{n-1}}{2n(n+1)w_\infty^2 - (n+1)w_\infty + 1} \right) \tilde{T}^n.$$

Note that the quantity \tilde{T} is related to T according to

$$\tilde{T} = \left(\frac{1 - \gamma\Omega_{\phi 0}}{1 - \Omega_{\phi 0}} \right) T,$$

which corresponds to a translation in N with the constant $-(1/3w_\infty) \ln[(1 - \gamma\Omega_{\phi 0})/(1 - \Omega_{\phi 0})]$.

As a next step Chiba [57] replaced \tilde{T} with $\tilde{T} = \Omega_\phi/(1 - \Omega_\phi)$, and expanded the resulting expression for w_ϕ in Ω_ϕ , which yields the following series, here truncated at second order, in Ω_ϕ :

$$w_\phi \approx w_\infty + \left(\frac{w_\infty(1 - w_\infty^2)}{4w_\infty^2 - 2w_\infty + 1} \right) \Omega_\phi \left[1 + \left(\frac{w_\infty(8w_\infty - 1)}{12w_\infty^2 - 3w_\infty + 1} \right) \Omega_\phi \right]. \quad (97)$$

Note that this is an expansion that is designed to improve the solution for the *linearized* equation for w_ϕ , *not* the actual solution of the *non-linear* equation for w_ϕ . The improved linear approximation only improves the actual solution to the extent the linear approximation describes that solution, which, fortunately, to some extent is the case for the inverse power law potential, see e.g., Figure 1 in [30]. However, not surprisingly, these approximations yield poorer accuracy than the present ones that are based on approximating the full non-linear equations.

B Scaling freezing quintessence

In [36] it was demonstrated that in appropriate variables, resulting in a global 3D state space setting, scaling freezing quintessence is associated with a single attractor orbit that constitutes the unstable manifold of an isolated fixed point. The situation and key attractor mechanism is thereby the same as for tracking quintessence. An open set of nearby orbits to the (hyperbolic) saddle fixed point is pushed toward the attractor orbit by a 2D invariant stable manifold boundary set, for details, see [36] and [37]. The difference with tracking quintessence is that scaling freezing quintessence arises from potentials that have an asymptotic exponential behaviour that is sufficiently steep.

We therefore consider the situation where $\lim_{\phi \rightarrow -\infty} \lambda = \lambda_-$, $\lambda_- > \sqrt{3}$, but where compatibility with nuclear synthesis data requires $\lambda_- \gg \sqrt{3}$, see [36] and references therein. Let us further assume that the scalar field, during the time epoch $N \in (-\infty, 0]$ for the attractor solution, rolls down a scalar field potential with $\lambda(\phi) > 0$ where $\lambda(\phi)$ is monotonically decreasing, i.e., we assume that

$$\Gamma = \frac{V V_{,\phi\phi}}{V_{,\phi}^2} = 1 + (\lambda^{-1})_{,\phi} > 1 \quad \text{and} \quad \lim_{\phi \rightarrow -\infty} \Gamma = 1. \quad (98)$$

For our analysis we will consider the dynamical system for the state space vector $(\lambda, \Sigma_\phi, \Omega_\phi)$, which can be obtained from (37):

$$\lambda' = -\sqrt{6}(\Gamma - 1)\lambda^2\Sigma_\phi, \quad (99a)$$

$$\Sigma'_\phi = -\frac{3}{2}(1 + \Omega_\phi - 2\Sigma_\phi^2)\Sigma_\phi + \sqrt{\frac{3}{2}}\lambda(\Omega_\phi - \Sigma_\phi^2), \quad (99b)$$

$$\Omega'_\phi = 3(\Omega_\phi - 2\Sigma_\phi^2)(1 - \Omega_\phi), \quad (99c)$$

where Γ now is considered to be a function of λ , i.e., $\Gamma = \Gamma(\lambda)$.

Before continuing, let us note that the simple example of a potential consisting of two exponential terms,

$$V = V_- e^{-\lambda_- \phi} + V_+ e^{-\lambda_+ \phi}, \quad \lambda_- > 0, \quad \lambda_- > \lambda_+, \quad V_\pm > 0, \quad (100)$$

yields

$$\Gamma = 1 + \frac{(\lambda_- - \lambda)(\lambda - \lambda_+)}{\lambda^2}. \quad (101)$$

In the present variables, scaling freezing quintessence is associated with the unstable manifold orbit that originates from the fixed point

$$S: \quad (\lambda, \Sigma_\phi, \Omega_\phi) = \left(\lambda_-, \sqrt{\frac{3}{2}} \left(\frac{1}{\lambda_-} \right), \frac{3}{\lambda_-^2} \right). \quad (102)$$

Next we assume that $\Gamma(\lambda)$ can be Taylor expanded around λ_- , i.e.,

$$\Gamma = 1 + \Gamma_1(\lambda - \lambda_-) + \frac{\Gamma_2}{2}(\lambda - \lambda_-)^2 + \dots, \quad \Gamma_n = \left. \frac{d^n \Gamma}{d\lambda^n} \right|_{\lambda=\lambda_-}. \quad (103)$$

Note that (101) is regular since $\lambda > \lambda_- > 0$ for the potential with two exponential terms and that

$$\Gamma_1 = -\left(\frac{\lambda_- - \lambda_+}{\lambda_-^2} \right), \quad \Gamma_2 = \frac{2(\lambda_- - 2\lambda_+)}{\lambda_-^3} \quad (104)$$

in this case.

We can now proceed in the same manner as for thawing and tracking quintessence and first make an expansion based on the unstable eigenvalue, $-3\lambda_- \Gamma_1$, which leads to expansions in

$$T = C e^{-3\lambda_- \Gamma_1 N}. \quad (105)$$

The fact that $\lim_{N \rightarrow -\infty} \Omega_\phi > 0$ and that the eigenvalue involves two parameters, λ_- and Γ_1 , result in quite messy expressions for the series expansions. For brevity we will therefore truncate the series already at the linear order in T :

$$\lambda = \lambda_- - T + \dots, \quad (106a)$$

$$\Sigma_\phi = \sqrt{\frac{3}{2}} \left(\frac{1}{\lambda_-} \right) (1 + \alpha T + \dots), \quad (106b)$$

$$\Omega_\phi = \frac{3}{\lambda_-^2} (1 + \beta T + \dots), \quad (106c)$$

where

$$\alpha = \frac{\lambda_-^3 \Gamma_1 + \lambda_-^2 - 3}{\lambda_- (2\lambda_-^4 \Gamma_1^2 - \lambda_-^3 \Gamma_1 + \lambda_-^2 - 3)}, \quad \beta = \frac{2(\lambda_-^2 - 3)}{\lambda_- (2\lambda_-^4 \Gamma_1^2 - \lambda_-^3 \Gamma_1 + \lambda_-^2 - 3)}. \quad (107)$$

Using that $w_\phi = -1 + 2\Sigma_\phi^2/\Omega_\phi$ yields

$$w_\phi = (2\alpha - \beta)T + \dots, \quad (108)$$

where

$$2\alpha - \beta = \frac{2\lambda_-^2 \Gamma_1}{\lambda_- (2\lambda_-^4 \Gamma_1^2 - \lambda_-^3 \Gamma_1 + \lambda_-^2 - 3)}. \quad (109)$$

Note that $\lim_{N \rightarrow -\infty} w_\phi = 0$, which leads to that asymptotically toward the past $\rho_\phi \propto \rho_m \propto a^{-3}$, hence the name *scaling freezing*, while w_ϕ decreases toward the future.

We leave the higher order series expansions, the construction of Padé approximants, the identification of C with present day data, and subsequent investigations, such as error estimates for various potentials, for the interested reader.

References

- [1] Supernova Search Team Collaboration: A. G. Riess et al. Observational evidence from supernovae for an accelerating universe and a cosmological constant. *Astron. J.*, **116**:1009, 1998.
- [2] Supernova Cosmology Project Collaboration: S. Perlmutter et al. Measurements of omega and lambda from 42 high redshift supernovae. *Astron. J.*, **517**:565, 1999.
- [3] DES Collaboration: T. M. C. Abbott et al. The dark energy survey: Cosmology results with 1500 new high-redshift type ia supernovae using the full 5-year dataset. *The Astrophysical Journal Letters*, 973(1), 2024.
- [4] Planck Collaboration: N. Aghanim et al. Planck 2018 results. vi. cosmological parameters. *Astron. Astrophys.*, 641 A6, 2020.
- [5] W. L. Freedman et al. The carnegie-chicago hubble program viii. an independent determination of the hubble constant based on the tip of the red giant branch. *The Astrophysical Journal*, 882(1):34, aug 2019.
- [6] A. G. Riess et al. Cosmic distances calibrated to 1% precision with gaia edr3 parallaxes and hubble space telescope photometry of 75 milky way cepheids confirm tension with λ cdm. *The Astrophysical Journal Letters*, 908(1):L6, feb 2021.
- [7] A. G. Riess et al. A comprehensive measurement of the local value of the hubble constant with 1 km s⁻¹ mpc⁻¹ uncertainty from the hubble space telescope and the sh0es team. *The Astrophysical Journal Letters*, 934(1):L7, jul 2022.
- [8] N. Menci et al. Constraints on dynamical dark energy models from the abundance of massive galaxies at high redshifts. *The Astrophysical Journal*, 900(2):108, sep 2020.

- [9] A. Almeida et al. The eighteenth data release of the sloan digital sky surveys: Targeting and first spectra from sdss-v. *The Astrophysical Journal Supplement Series*, 267(2):44, aug 2023.
- [10] S. Alam et al. The clustering of galaxies in the completed sdss-iii baryon oscillation spectroscopic survey: cosmological analysis of the dr12 galaxy sample. *Monthly Notices of the Royal Astronomical Society*, 470(3):2617–2652, 03 2017.
- [11] J. Hou et al. The completed sdss-iv extended baryon oscillation spectroscopic survey: Bao and rsd measurements from anisotropic clustering analysis of the quasar sample in configuration space between redshift 0.8 and 2.2. *Monthly Notices of the Royal Astronomical Society*, 500(1):1201–1221, 10 2020.
- [12] S. Alam et al. Completed sdss-iv extended baryon oscillation spectroscopic survey: Cosmological implications from two decades of spectroscopic surveys at the apache point observatory. *Phys. Rev. D*, **103(8)**:083533, 2021.
- [13] DESI Collaboration: A. G. Adame et al. Desi 2024 vi: cosmological constraints from the measurements of baryon acoustic oscillations. *Journal of Cosmology and Astroparticle Physics*, 2025(02):021, feb 2025.
- [14] M. Ishak et al. Modified gravity constraints from the full shape modeling of clustering measurements from desi 2024. *FERMILAB-PUB-24-0848-PPD*, 2024.
- [15] DESI Collaboration: A. G. Adame et al. Desi 2024 vii: Cosmological constraints from the full-shape modeling of clustering measurements. *arXiv:2411.12022v2*, 2024.
- [16] V. C. Rubin et al. Rotation of the andromeda nebula from a spectroscopic survey of emission regions. *Astrophys. J.*, 159:379, feb 1970.
- [17] V. Trimble. Existence and nature of dark matter in the universe. *Annual Rev. Astron. Astrophys.*, 25:425–472, jan 1987.
- [18] M. Tegmark et al. Cosmological parameters from sdss and wmap. *Phys. Rev. D*, 69:103501, May 2004.
- [19] Ryan E et al. Keeley. Jwst lensed quasar dark matter survey – ii. strongest gravitational lensing limit on the dark matter free streaming length to date. *Monthly Notices of the Royal Astronomical Society*, 535(2):1652–1671, 11 2024.
- [20] D. H. Weinberg et al. Cold dark matter: Controversies on small scales. *Proceedings of the National Academy of Sciences*, 112(40):12249–12255, feb 2015.
- [21] J. S. Bullock and M. Boylan-Kolchin. Small-scale challenges to the λ cdm paradigm. *Annual Review of Astronomy and Astrophysics*, 55:343–387, 2017.
- [22] P. J. E. Peebles and Bharat Ratra. The cosmological constant and dark energy. *Rev. Mod. Phys.*, **75**:559–606, 2003.

- [23] DES Collaboration: T. M. C. Abbott et al. Dark energy survey year 1 results: Cosmological constraints from cluster abundances and weak lensing. *Phys. Rev. D*, 102:023509, Jul 2020.
- [24] A. G. Riess et al. Large magellanic cloud cepheid standards provide a 1% foundation for the determination of the hubble constant and stronger evidence for physics beyond λ cdm. *The Astrophysical Journal*, 876(1):85, may 2019.
- [25] E. Di Valentino et al. In the realm of the hubble tension: a review of solutions. *Classical and Quantum Gravity*, 38(15):153001, jul 2021.
- [26] Le Conte et al. A jwst investigation into the bar fraction at redshifts $1 \leq z \leq 3$. *Monthly Notices of the Royal Astronomical Society*, 530(2):1984–2000, 04 2024.
- [27] M. Chevallier and D. Polarski. Accelerating universes with scaling dark matter. *Int. J. Mod. Phys.*, **D10**:213, 2001.
- [28] E.V. Linder. Exploring the expansion history of the universe. *Phys. Rev. Lett.*, **90**:091301, 2003.
- [29] V. Sahni and A. Starobinsky. Reconstructing dark energy. *International Journal of Modern Physics D*, 15(12):2105–2132, jan 2006.
- [30] S. Tsujikawa. Quintessence: a review. *Class. Quantum Grav.*, **30**:214003, 2013.
- [31] O. Avsajanishvili et al. Observational constraints on dynamical dark energy models. *Universe*, 10(3:122), 2024.
- [32] William J. Wolf and Pedro G. Ferreira. Underdetermination of dark energy. *Phys. Rev. D*, 108:103519, Nov 2023.
- [33] David Shlivko and Paul J. Steinhardt. Assessing observational constraints on dark energy. *Physics Letters B*, 855:138826, 2024.
- [34] A. Alho and C. Uggla. Global dynamics and inflationary center manifold and slow-roll approximants. *Journal of Mathematical Physics*, **56**(012502), 2015.
- [35] R. R. Caldwell and E. V. Linder. Limits of quintessence. *Phys. Rev. Lett.*, **95**:141301, 2005.
- [36] A. Alho, C. Uggla, and J. Wainwright. Quintessence from a state space perspective. *Physics of the Dark Universe*, **39**:101146, 2023.
- [37] A. Alho, C. Uggla, and J. Wainwright. Tracking quintessence. *Physics of the Dark Universe*, **44**:101433, 2024.
- [38] A. Alho and C. Uggla. Quintessential α -attractor inflation: A dynamical systems analysis. *Journal of Cosmology and Astroparticle Physics*, **11**:083, 2023.
- [39] A. A. Coley, J. Ibáñez, and R. J. van den Hoogen. Homogeneous scalar field cosmologies with an exponential potential. *Journal of Mathematical Physics*, 38:17, 1997.

- [40] E. J. Copeland, A. R. Liddle, and D. Wands. Exponential potentials and cosmological scaling solutions. *Phys. Rev. D*, **57**:4686, 1998.
- [41] L. A. Urena-Lopez. Unified description of the dynamics of quintessential scalar fields. *JCAP*, **2012**:035, 2012.
- [42] A. Alho and C. Uggla. Scalar field deformations of lambda-cdm cosmology. *Phys. Rev. D*, **92**(10):103502, 2015.
- [43] J. Wainwright and G. F. R. Ellis. *Dynamical systems in cosmology*. Cambridge University Press, 1997.
- [44] P. J. E. Peebles and B. Ratra. Cosmology with a time variable cosmological constant. *Astro. Phys. J.*, **325**:L17, 1988.
- [45] B. Ratra and P. J. E. Peebles. Cosmological consequences of a rolling homogeneous scalar field. *Phys. Rev. D*, **37**:3406, 1988.
- [46] B. Ratra and A. Quillen. Gravitational lensing effects in a time-variable cosmological ‘constant’ cosmology. *Monthly Notices of the Royal Astronomical Society*, **259**(4):738–742, 12 1992.
- [47] I. Zlatev, L. Wang, and P. J. Steinhardt. Quintessence, cosmic coincidence and the cosmological constant. *Phys. Rev. Lett.*, **82**:896, 1999.
- [48] P. J. Steinhardt, L. Wang, and I. Zlatev. Cosmological tracking solutions. *Phys. Rev. D*, **59**:123504, 1999.
- [49] S. Podariu and B. Ratra. Supernova ia constraints on a time-variable cosmological constant. *The Astrophysical Journal*, **532**(1):109, mar 2000.
- [50] V. Sahni and A. Starobinsky. The case for a positive cosmological lambda-term. *Int. J. Mod. Phys. D*, **9**:373, 2000.
- [51] L.A. Urena-Lopez and T. Matos. New cosmological tracker solution for quintessence. *Phys. Rev. D*, **62**:081302, 2000.
- [52] K. Dimopoulos and C. Owen. Quintessential inflation with α -attractors. *J. of Cosmology and Astroparticle Physics*, **06**:027, 2017.
- [53] Y. Akrami et al. Dark energy, α -attractors, and large-scale structure surveys. *JCAP*, **06**:041, 2018.
- [54] Y. Akrami et al. Quintessential α -attractor inflation: forecasts for stage iv galaxy surveys. *JCAP*, **04**:006, 2021.
- [55] R. J. Scherrer and A. A. Sen. Thawing quintessence with a nearly flat potential. *Phys. Rev. D*, **77**:083515, Apr 2008.
- [56] T. Chiba. Slow-roll thawing quintessence. *Phys. Rev. D*, **79**:083517, 2009.
- [57] T. Chiba. Equation of state of tracker fields. *Phys. Rev. D*, **81**:023515, 2010.

- [58] M. Raveri, W. Hu, and S. Sethi. Swampland conjectures and late-time cosmology. *Phys. Rev. D*, **99**:083518, Apr 2019.
- [59] P. Agrawala, G. Obieda, P. J. Steinhardt, and C. Vafa. On the cosmological implications of the string swampland. *Physics Letters B*, **784**:271, 2018.
- [60] R. N. Cahn, R. de Putter, and E. V. Linder. Field flows of dark energy. *Journal of Cosmology and Astroparticle Physics*, **2008**(11):015, nov 2008.
- [61] S. Dutta and R. J. Scherrer. Hilltop quintessence. *Phys. Rev. D*, **78**:123525, Dec 2008.
- [62] R. Crittenden, E. Majerotto, and F. Piazza. Measuring deviations from a cosmological constant: A field-space parametrization. *Phys. Rev. Lett.*, **98**:251301, Jun 2007.
- [63] C. R. Watson and R. J. Scherrer. Evolution of inverse power law quintessence at low redshift. *Phys. Rev. D*, **68**:123524, 2003.